International Conference on Mechanical Engineering 2015
(ICME 2015) 18 – 20 December, 2015, Dhaka, Bangladesh

Paper ID : K-01

1D Network Simulation of Blood Flow in the Circle of Willis

P. G. Huang[1, a)], H. Yu[1], Z. Yang[1], B. Ludwig[2, 3]

[1]*Department of Mechanical and Materials Engineering, Wright State University, Dayton, OH 45435*
[2]*Wright State University Boonshoft School of Medicine, Wright State University, Dayton, OH 45435*
[3]*Department of Neurology – Division of Neuro Interventional Surgery, Wright State University / Premier Health - Clinical Neuroscience Institute, 30 E. Apple St, Dayton OH 45409*

[a)]Corresponding author: george.huang@wright.edu

Abstract. A 1D simulation of the complete vessel network, THINkS (Total Huma Intravascular Network Simulation), is introduced to study the effect of blood regulation due to the circle of Willis (CoW) anomaly. A comparison of the complete CoW and an incomplete CoW anomaly has suggested the ring-like vessel connection may regulate the blood flow to enable different parts of brain to receive the same blood flow rates. The regulation mechanism is built into the ring-like structure and requires no external stimuli. Due to this auto-regulation, the flow pattern in CoW may vary significantly and a careful investigation of the flow patterns caused by the CoW anomaly may help us understand the initiation, development, and risk management of the cerebral aneurysms.

INTRODUCTION

The circle of Willis (CoW), as shown in Figure 1, is a ring like arterial structure at the base of the brain. Blood is supplied to the brain through two internal carotid arteries (ICAs) and the basilar artery (BA). Each ICA divides into the middle cerebral artery (MCA) and anterior cerebral artery (A-1s and A-2s) to perfuse the temporal, parietal and frontal regions of the brain.

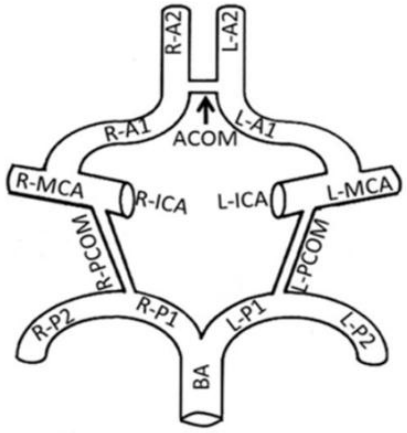

FIGURE 1. Circle of Willis. A1 and A2: anterior cerebral artery 1 and 2; MCA: middle cerebral artery; P1 and P2: posterior cerebral artery 1 and 2; ICA: internal carotid artery; BA: Basilar artery; ACOM: anterior communication artery; PCOM: posterior communication artery.

The left and right anterior cerebral arteries are connected by the anterior communicating artery (ACOM) to form the anterior circulation. In contrast, BA branches into the right and left posterior cerebral arteries (P-1s and P-2s) to deliver blood to the regions of the brain stem, termed the posterior circulation. The anterior and the posterior circulations are interconnected by the posterior communicating arteries (PCOMs). This resulting ring-like arterial structure is the main collateral pathway in the cerebral circulation and most of the cerebral aneurysms are found in the region. The CoW provides multiple paths for oxygenated blood to supply the brain if any part of circle are constricted by birth defect, occluded by disease, or interrupted by injury. It was suggested that approximate 60% of the populations do not hold a complete CoW [1]. Recent evidence has shown that the flow pattern in the CoW may be affected greatly as a result of compensating effects (auto-regulation) to redistribute the blood flow and these effects may be highly asymmetric [2, 3].

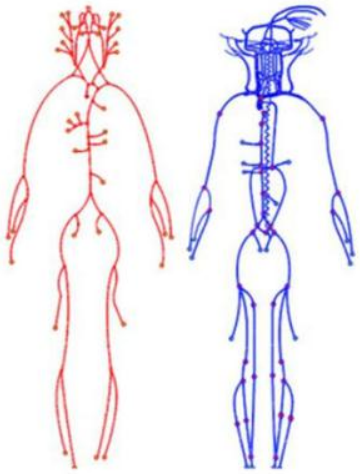

FIGURE 2. Human's vessel network - arteries are red and veins are blue.

In this study, a 1D simulation of the vessel network is provided to investigate the changes of flow patterns caused by an anomaly type of missing A1 artery in the CoW. The method is based on 1D network simulation of a complete human blood circulation [3, 4] and it has been extensively tested in Muller and Toro [4] and Huang and Muller [3]. Our intent is to use this approach to recognize the alteration of flow patterns caused by the variation in the CoW and to identify the role of fluid flow involved in the formation and eventual rupture of intracerebral aneurysms.

METHODS

0D-1D Network Approach

The 0D-1D network simulation of the complete human circulatory system including major arteries, veins, and 0D models for the heart and different human organs has been published [3, 4]. The blood flow in major arteries (red network) and veins (blue network) as shown in Figure 1 is represented by the 1D hemodynamic equations derived from conservations of mass and momentum, and a wall law to relate variations in cross-sectional area to variations in local pressure [5]. The resistance due to the major (friction) and minor (curvature, stenosis, bend, and circulation) losses can be included empirically by adding them as source terms in the momentum equation. The solution method is similar to the conventional numerical schemes used for gas dynamic equations. In this case a high order TVD scheme is proposed [3].

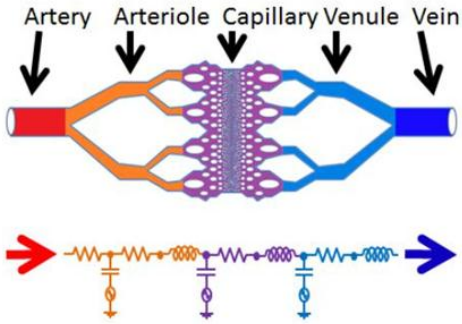

FIGURE 3. 0D model for micro-circulation.

The treatment for the microcirculation is slightly more empirical. The major arteries branch into arterioles. Arterioles then become so small as to form capillaries, allowing the diffusion of oxygen and nutrients from the blood into tissues, and diffusion of waste products of the metabolism from the tissues into the blood. On the venous end, capillaries merge to form a venule. Venules are the smallest veins collecting blood to the major veins. Figure 2 shows a simple illustration of the microcirculation model for the blood flow in the kidney. The blood enters and leaves the kidney through the renal artery and the renal vein, respectively. The arteriole, capillary, and venule are each represented by an RLC circuit. The relationship between the RLC circuit and the 1D hemodynamic equations was established in [6], and the values for resistors (R), inductors (L) and capacitors (C) can be found in literatures [3, 4, 7].

THINkS (Total Human Intravascular Network Simulation)

The tool we used in this study is based on an in-house computer program – THINkS. THINkS consists of a simulation of 85 major arteries, 158 major veins, 43 arterial and 77 venous junctions. Blood flow in arterioles, capillaries and venules is modeled using lumped parameter models, or the 0D models, which are modeled using the connection of a number of capacitors, resistors and inductors to represent the real physics. The model used a simple 0D model for 20 one-artery-to-one-vein micro- circulations and 4 other 0D models for 7 complex arteries-to-veins micro-circulations. Moreover, a 4-chamber 0D model for the heart is used to allow blood to pump from the superior vena cava and inferior vena cava veins, through the pulmonary system, and discharge back to the ascending aorta artery. In addition to the 4 valves inside the heart, there are also 15 venous valves used in the venous system. The tool is constructed in such a way that blood vessels can be easily added or deleted as needed. Hence, it is completely customizable based on patients' conditions and their medical needs. The physiological data for the subject discussed in this study can also be found in the original papers [3, 4].

Circle of Willis Anomaly

Many studies have been focused on the linkage between CoW anomaly and risk management of aneurysms. Unfortunately, this linkage may be difficult to establish without the knowledge of the flow pattern changes caused by the anomaly. This study shows how the flow in CoW is regulated under an anomaly type of missing A1 artery, as depicted in Figures 4 (a) and (c), corresponding to the missing right and left A1 types, respectively. Our objective is to compare these cases with the complete CoW type and demonstrate the importance of flow migration resulting from such anatomical anomalies.

RESULTS AND DISCUSSION

Flow Pattern of a Complete CoW

The blood flow rate distribution for the complete CoW is shown Figure 4 (b). As can be seen from the figure, the blood is supplied to the CoW through two internal carotid arteries (ICAs) and the basilar artery (BA) and it exits from two anterior cerebral arteries (A2's) , two middle cerebral arteries; (MCA's) and two posterior cerebral arteries (P2's). The results showed the predicted averaged flow rate in each of ICAs is approximately 270 ml/min. This value is between the ones reported clinically by Hendriskse et al. [2] and by Tanaka et al. [8], 245 ± 65 ml/min and 305 ± 74 ml/min, respectively. The predicted averaged flow rate of BA is 130 ml/min. Again the result is between the values reported by Hendriskse et al. [2] and by Tanaka et al. [8], 118 ± 37 ml/min and 165 ± 43 ml/min, respectively. It should be noted that Tanaka et al. and Hendriskse et al. both showed roughly the same percentage of flow rate for ICA and BA: 80% and 20%, respectively [2, 8]. The current computation also agrees with this observation very well.

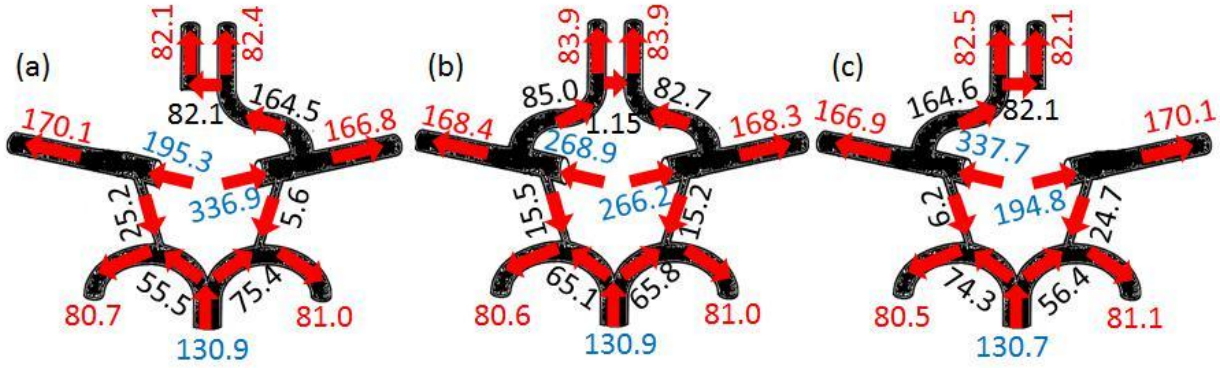

FIGURE 4. Averaged flow rate distributions for the missing-A1 CoW variations, in ml/min. Blue is afferent vessels and red is efferent vessels. (a) missing right A1 type, (b) the complete type and (c) the missing left A1 type.

Flow Pattern of the CoW Variations

Figure 4 depicts the flow rate comparisons of the missing-A1 CoW anomalies with the complete CoW . The total flow rates for the complete, the missing right-A1 and missing left A1 types are: 666.0, 663.1 and 663.2 ml/min, respectively and they are virtually unaffected by the variations. Moreover, the flow rates of the efferent arteries only changed slightly while those of the afferent vessels may alter substantially. The "ring like" structure of the CoW has been hypothesized to have the ability to perfuse deprived areas when a patient is missing one of the main arteries or due to complete or partial occlusion of one of the arteries. However, this autoregulation was believed to be caused by dilation and constriction of the arterioles in response to different environmental stimuli [9]. In the engineering discipline, this type of regulation is often referred to an active control. The computational evidence, however, shows that the autoregulation of the CoW is a built-in mechanics associated with its ring-like structure and it requires no external stimuli. Hence, the auto-regulation should be considered as a passive control as defined in the engineering discipline.

A Possible Connection Between the Missing A-1 Cow Anomaly and ACOM Aneurysms

Although the CoW variations shown above do not seem to cause an immediate threat because the blood supply to different parts of the human brain is almost unaffected, these variations may have a long term effect to the initiation, development, and rupture of the intracranial aneurysms. Using our calculations, it would appear

redistribution of the flow through the CoW may cause specific CoW vessels to carry excessive load and the high flow rate may stress the wall of the artery in that region and hence leads to a high probability of an aneurysm in that region. For example, Figures 4 (a) and 4(b) show that the missing A1 variation may cause the flow rate in the ipsilateral ICA to increase from 266 ml/min to 337 ml/min while the flow rate in the contralateral ICA is reduced by the same amount. The ACOM is then responsible for shunting the imbalanced blood flow from the ipsilateral A1 to the contralateral A2. As a result, the flow rate in the ACOM is substantially changed -- from 1.15 ml/min to a reverse flow of 82.1 ml/min (and in the case of missing left-A1type to 82.1 ml/min in the same direction). Because the wall shear stress is proportional to the mean velocity based on the theory of pipe flow, the wall of ACOM in the missing A1 types is subject to an excessively large shear force as compared to the case with complete CoW. Hence, one is more likely to observe ACOM aneurysm when subject to a missing A1. Our hypothesis is somewhat supported by a recently clinical study where it was concluded that variation in the A1 segment is correlated with a higher prevalence of ACOM aneurysms compared with patients with a complete CoW [10].

CONCLUDING REMARKS

The blood regulation in the circle of Willis was simulated by a 1D network computational tool, THINkS. The CoW anomalies of missing A1 were investigated numerically and results confirmed that the total blood flow to the CoW is insensitive to the missing A1 anomaly. The study also demonstrated that the CoW is capable of regulating the blood to the deprived area to avoid the symptoms of ischemia without needing other external stimuli. Hence this auto-regulation mechanism is built into the ring-like structure and the control is a passive one. This study further suggested that the change of flow pattern caused by the CoW anomaly may result in excessive load in certain vessel region and this may lead to some justifications to the association of the locations of aneurysms with the CoW anomaly.

REFERENCES

1. J. C. Lasheras , Annu. Rev. Fluid Mech **39**, 293-319 (2007).
2. J. Hendrikse, A. F. van Raamt, Y. van der Graaf , W. P. Mali, J. van der Grond, Radiology **235,** 184-9, (2005).
3. P. G. Huang and L. O. Muller, Int J for Numer Meth in Biomed Eng **31(5)**, p. e02701, (2015).
4. L. O. Muller, E. F. Toro, Int. J. for Numer. Meth. in Biomed. Eng **30(7)**, 681-725 (2014).
5. S.J. Sherwin, V. Franke, J. Peiró, K. Parker, J Eng Mathem **47**, 217-250 (2003).
6. J. Alastruey, K. H. Parker, J. Peiro, S. J. Sherwin, Commu in Comput Phys **4(2)**, 317-336 (2008).
7. F. Liang, S. Takagi, R. Himeno, H. Liu, Med Biol Eng Comput **47(7)**, 743-755. (2009).
8. H. Tanaka, N. Fujita, T. Enoki, K. Matsumoto , Y. Watanabe, K. Murase, H. Nakamura, Am J. Neuroradiol **27**, 1770-1775 (2006).
9. J. Alastruey, K. H. Parker, J. Peiro, S. M. Byrd, S. J. Sherwin, J. of Biomechanics **40**, 1794-1805 (2007).
10. A. Krasny, F. Nensa, I. E. Sandalcioglu, S. L. Göricke, I. Wanke, C. Gramsch, S. Sirin, N. Oezkan, U. Sure, M. Schlamann, J Neurointerv Surg **6**, 178-83 (2014).

ICME2015

International Conference on Mechanical Engineering 2015
(ICME 2015) 18 – 20 December, 2015, Dhaka, Bangladesh

Paper ID : K-02

Nuclear for Climate Change: Safety First, Last and Always

Kune Y. Suh

Professor of Nuclear Engineering, Seoul National University, Seoul 08826, Republic of Korea
President, Philosophia Inc., Seoul National University, Seoul 08826, Republic of Korea
Chairman, Korea Atomic Safety Protection Institution, Seoul National University, Seoul 08826, Republic of Korea
kysuh@snu.ac.kr, kysuh@alum.mit.edu

Abstract. The nuclear waste produced during the fission process, such as the water used to cool the reactor and the spent fuel, are radioactive. Since it can take thousands of years for radioactive level of these materials to reduce to a safe level for humans and the environment, the waste must be stored in a secure place. If not, the high levels of radiation can hurt the living and the surrounding environment. People against nuclear are also worried about safety. Should something go wrong mechanically, or a natural disaster hit, that radiation can be released into the atmosphere, such as what happened in Chernobyl and Fukushima. Nuclear power is nonetheless considered to be resourceful. The heat released from 1 g of uranium is equivalent to burning about 3 tons of coal or more than 12 barrels of oil. It is a sustainable energy source that reduces carbon emissions. Furthermore, this means that even after the cost of building the nuclear power plant, using nuclear power is still more cost effective than coal or gas-fired power plants. Nuclear is clearly on its way back to sustaining civilization well into the next century, if not millennium, together with renewables.

NUCLEAR TOWARDS LOW-CARBON SOCIETY

It is considered that nuclear energy is indeed a key part of the solution to limiting climate change, and that the world must use all low-carbon energy sources, including nuclear, if it is to limit climate change while still meeting the development goals. The global challenge is huge. By 2050, 80% of global electricity will have to be produced with low-carbon technology compared against 30% now so as to cope with climate change. [1] During the same period, global demand for electricity may as well double to meet the crucial needs of humanity in terms of population growth and development goals.

Also, low-carbon electricity is expected to play a key role in decarbonizing other sectors. [2] This challenge requires the use of all low-carbon energy technologies: renewables, nuclear, and fossil fuels with carbon capture and sequestration, and underscores the need for large-scale low- or no-carbon electric generation options. It is recognized that the life cycle greenhouse gas emissions per kWh from nuclear power plants are two orders of magnitude lower than those of fossil fuel and comparable to most renewables.

A significant part of the CO_2 released remains in the atmosphere for a long period of time. We need to start reducing CO_2 emissions now to slow down the increase in concentration. Energy transitions take decades to implement. We need to leverage the full range of low-carbon energy options available today while continuing to develop advanced technologies that can be implemented by 2050. Nuclear is clearly one of the few currently available energy options that has already proven to be effective and can be implemented on a large scale.

Pathways with the greatest probability for successfully decarbonizing the energy mix require the use of nuclear energy, like it or not. Countries must meet climate goals and at the same time meet other energy policy objectives. Nuclear energy enables countries to reduce CO_2 emissions while helping to improve energy security, providing affordable electricity, and facilitating economic and industrial development.

NUCLEAR SAFETY, SECURITY AND SAFEGUARDS

In the 1950s attention had turned to harnessing the power of the atom in a controlled way, which culminated in demonstration at Chicago in 1942. The so-called chain reaction was mistakenly deployed for military purposes. The civilian effort was then poured to applying the steady heat yield to generate electricity. This naturally gave rise to concerns about accidents and their possible consequences. Nuclear safety depends on intelligent planning, proper design with conservative margins and backup systems, high-quality components and a well-developed safety culture in operations and maintenance.

When it comes to nuclear, safety is associated with security and safeguards as well. [3] First and foremost, safety focuses on unintended conditions or events leading to radiological releases from authorized activities. It relates mainly to intrinsic problems or hazards. Security looks to the intentional misuse of nuclear or other radioactive materials by non-state elements to cause harm. It relates largely to external threats to materials or facilities. Safeguards have to do with restraining activities by states that could lead to acquisition of nuclear weapons. They concern materials and equipment in relation to rogue governments.

An accident scenario of particular interest and keen attention was loss of cooling which resulted in melting of the nuclear reactor core. This triggered studies on both the physical and chemical possibilities as well as the biological consequences of any dispersed radioactivity. Those responsible for developing nuclear technology in the West devoted extraordinary effort to ensuring that a meltdown of the reactor core would not take place, since it was assumed that a meltdown of the core would create a major public hazard, and if uncontained, a tragic accident with likely multiple fatalities.

There has been a sturdy alertness for the potential hazard of both nuclear criticality and release of radioactive materials from nuclear power plants. As in other industries, the design and operation of nuclear power plants aim to minimize the likelihood of accidents, and to avoid major human as well as environmental consequences when they do happen to occur. The consequences of an accident or terrorist attack must be kept minimal compared with other commonly accepted risks.

There have thus far been three major reactor accidents in the history of civil nuclear power – Three Mile Island, Chernobyl and Fukushima. TMI was contained without harm to anyone, Chernobyl involved an intense fire without provision for containment, and Fukushima relentlessly tested the containment, allowing considerable release of radioactivity. They turned out to be the most severe accidents during 16,000 cumulative reactor-years of commercial nuclear power operation in 33 countries. [3]

Of all the accidents and incidents, only the Chernobyl and Fukushima resulted in radiation doses to the public greater than those resulting from the exposure to natural sources. The Fukushima accident resulted in some radiation exposure of workers at the plant, but not such as to threaten their health, unlike Chernobyl. The TMI accident and other incidents have been completely confined to the plant.

Apart from Chernobyl, no nuclear workers or members of the public have ever died from exposure to radiation due to a commercial nuclear reactor incident. Most of the serious radiological injuries and deaths that occur each year tantamount to 2-4 deaths and many more exposures above regulatory limits result from large uncontrolled radiation sources such as abandoned medical or industrial equipment. In fact, there have also been a number of accidents in experimental reactors and in one military plutonium-producing pile – at Windscale, UK, in 1957, but none of these resulted in loss of life outside the actual plant, or long-term environmental contamination. [3]

A commercial nuclear reactor simply cannot under any circumstances go off like a bomb – the fuel is not enriched beyond 5%, and much higher enrichment, say 90%, is needed for explosives. The International Atomic Energy Agency was set up by the United Nations in 1957. One of its functions was to act as an auditor of world nuclear safety, and this role was increased greatly following the Chernobyl accident. It prescribes safety procedures and the reporting of even minor incidents. Its role has been strengthened since 1996. Every country which operates nuclear power plants has a nuclear safety inspectorate all of whom work closely with the Agency.

HOW SAFE IS SAFE ENOUGH

A fundamental principle of nuclear power plant operation worldwide is that the operator is responsible for safety. The national regulator is responsible for ensuring the plants are operated safely by the licensee, and that the design is approved. There is international collaboration among these to varying degrees. Also, there are a number of sets of mechanical codes and standards related to quality and safety.

With new reactor designs being established on a more international basis since the 1990s, both industry and regulators are seeking greater design standardization and also regulatory harmonization. Note that the theoretically-calculated frequency for a large release of radioactivity from a severe accident has been reduced by a factor of 1600 between the early Generation I reactors as originally built and the Generation III/III+ plants being built today. Earlier designs however have been progressively upgraded through their operating lives.

It has long been asserted that reactor accidents are the epitome of low-probability but high-consequence risks. Understandably, some were disinclined to accept the risk, however low the probability may be. Yet, the physics and chemistry of a reactor core, coupled with but not wholly depending on the engineering, mean that the consequences of an accident are likely in fact be much less severe than those from other industrial and energy sources. Experience, including Fukushima, bears this out.

About 80% of all events are attributed to human error. In some industries, this number is closer to 90%. Roughly 20% of occurrences involve equipment failures. When the 80% human error is broken down, the majority of errors associated with events stem from latent organizational weaknesses committed by humans in the past that lie dormant in the system. About 30% are caused by the individual worker touching the equipment and systems in the facility. Clearly, focusing efforts on reducing human error will reduce the likelihood of occurrences and events. Following the Fukushima accident the focus has been on the organizational weaknesses which increase the likelihood of human error.

Be reminded that the safety record of the US Navy from 1955 on is excellent, this being attributed to a high level of standardization in over one hundred naval power plants and in their maintenance, and the high quality of the Navy's training program. Until the 1980s, the Soviet naval record stood in marked contrast.

DEFENSE IN DEPTH

To achieve optimum safety, nuclear plants in the western world operate based on a 'defence-in-depth' approach, with multiple safety systems supplementing the natural features of the reactor core. Key aspects of the approach can be summed up as prevention, monitoring, and action to mitigate consequences of failures. They include, but are not limited to, high-quality design and construction, equipment which prevents operational disturbances or human failures and errors developing into problems, comprehensive monitoring and regular testing to detect equipment or operator failures, redundant and diverse systems to control damage to the fuel and prevent significant radioactive releases, and provision to confine the effects of severe fuel damage to the plant itself.

The safety provisions include a series of physical barriers between the radioactive reactor core and the environment, the provision of multiple safety systems, each with backup and designed to accommodate human error. Safety systems account for about one quarter of the capital cost of such reactors. As well as the physical aspects of safety, there are institutional aspects which are no less important.

The fuel is in the form of solid ceramic pellets, and radioactive fission products remain largely bound inside the pellets as the fuel is burned. The pellets are packed inside sealed zirconium alloy tubes or cladding to form fuel rods. These are confined inside a large steel pressure vessel with walls up to 30 cm thick. All this, in turn, is enclosed inside a robust reinforced concrete containment structure with walls at least 1 m thick. This amounts to three significant barriers around the fuel, which itself is stable up to very high temperatures.

These barriers are monitored continually. The cladding is monitored by measuring the amount of radioactivity in the coolant water. The pressure boundary is monitored by the leak rate of water, and the containment structure by periodically measuring the leak rate of air at about five times the atmospheric pressure.

The three basic safety functions in a reactor are to control reactivity, to cool the fuel and to contain radioactive substances. The main safety features of most reactors are inherent - negative temperature coefficient and negative void coefficient. The first means that beyond an optimal level, as the temperature increases the efficiency of the reaction decreases. The second signifies that if any steam has formed in the coolant water there is a decrease in moderating effect so that fewer neutrons can cause fission and the reaction slows down automatically.

In the 1950s and 1960s some experimental reactors in Idaho were deliberately tested to destruction to verify that large reactivity excursions were self-limiting and would automatically shut down the fission reaction. These tests verified that this was indeed the case. Beyond the control rods which are inserted to absorb neutrons and regulate the fission process, the main engineered safety provisions are the backup emergency core cooling system to remove excess heat and the containment.

Traditional reactor safety systems are active in the sense that they involve electrical or mechanical operation on command. Some engineered systems operate passively like pressure relief valves. Both require parallel redundant systems. Inherent or full passive safety design depends only on physical phenomena such as convection, gravity or resistance to high temperatures, not on functioning of engineered components. All reactors have some elements of inherent safety as mentioned above, but in some recent designs the passive or inherent features substitute for active systems in cooling. Such a design would have averted the Fukushima accident, where loss of electrical power resulted is loss of cooling function.

The basis of design assumes a threat where due to accident or malign intent such as terrorism there is core melting and containment failure. This double possibility has been well studied and provides the basis of exclusion zones and contingency plans. Apparently during the Cold War neither the USSR nor the USA targeted the other's nuclear power plants because the likely damage would be modest.

Nuclear power plants are designed with sensors to shut down automatically in an earthquake, and this is a vital consideration in many parts of the world.

SEVERE ACCIDENT MANAGEMENT

In both the TMI and Fukushima accidents the problems started after the reactors were shut down – immediately at TMI and after an hour at Fukushima, when the tsunami landed. The need to remove decay heat from the fuel was not met in each case, so core melting started to occur within a few hours. Cooling requires water circulation and an external heat sink. If pumps cannot run due to lack of power, gravity must be relied upon, but this will not get water into a pressurised system – either reactor pressure vessel or containment. Hence there is provision for relieving pressure, sometimes with a vent system, but this must work and be controlled without power.

There is a question of filters or scrubbers in the vent system: these need to be such that they do not block due to solids being carried. Ideally any vent system should deal with any large amounts of hydrogen, as at Fukushima, and have minimum potential to spread radioactivity outside the plant. Filtered containment ventilation systems are being retrofitted to some reactors which did not already have them, or any of sufficient capacity, following the Fukushima accident. The basic premise is that, independent of the state of the reactor itself, the catastrophic failure of the containment structure can be avoided by discharging steam, air and incondensable gases like hydrogen to the atmosphere.

The TMI accident revealed the importance of the inherent safety features. Despite the fact that about half of the reactor core melted, radioactive materials released from the melted fuel mostly plated out on the inside of the plant or dissolved in condensing steam. The containment building which housed the reactor further prevented any significant release of radioactivity. The accident was attributed to mechanical failure and operator confusion. The

reactor's other protection systems also functioned as designed. The emergency core cooling system would have prevented any damage to the reactor but for the intervention of the operators.

Investigations following the accident led to a new focus on the human factors in nuclear safety. No major design changes were called for in western reactors, but controls and instrumentation were improved significantly and operator training was overhauled.

At Fukushima Daiichi in 2011 the three operating reactors shut down automatically, and were being cooled as designed by the normal residual heat removal system using power from the backup generators, until the tsunami swamped them an hour later. The emergency core cooling systems then failed. Days later, a separate problem emerged as spent fuel ponds lost water. Analysis of the accident showed the need for more intelligent siting criteria than those used in the 1960s, and the need for better backup power and post-shutdown cooling, as well as provision for venting the containment of that kind of reactor and other emergency management procedures.

Nuclear plants have Severe Accident Management Guidelines, and most of these address what should be done for accidents beyond design basis, and where several systems may be disabled.

In 2007 the US NRC launched a research program to assess the possible consequences of a serious reactor accident. Its draft report was released nearly a year after the Fukushima accident had partly confirmed its findings. The State-of-the-Art Reactor Consequences Analysis showed that a severe accident at a US nuclear power plant would not be likely to cause any immediate deaths, and the risks of fatal cancers would be vastly less than the general risks of cancer.

Its most important conclusions fall into three areas: how a reactor accident progresses; how existing systems and emergency measures can affect an accident outcome; and how an accident would affect the public health. The principal conclusion is that existing resources and procedures can stop an accident, slow it down or reduce its impact before it can affect the public, but even if accidents proceed without such mitigation they take much longer to happen and release much less radioactive material than earlier analyses suggested. This was borne out at Fukushima, where there was ample time for evacuation – three days – before any significant radioactive releases.

In 2015 the Canadian Nuclear Safety Commission released its Study of Consequences of a Hypothetical Severe Nuclear Accident and Effectiveness of Mitigation Measures. This was the result of research and analysis undertaken to address concerns raised during public hearings in 2012 on the environmental assessment for the refurbishment of Ontario Power Generation's Darlington nuclear power plant. The study involved identifying and modelling a large atmospheric release of radionuclides from a hypothetical severe nuclear accident at the four-unit Darlington power plant; estimating the doses to individuals at various distances from the plant, after factoring in protective actions such as evacuation that would be undertaken in response to such an emergency; and, finally, determining human health and environmental consequences due to the resulting radiation exposure. It concluded that there would be no detectable health effects or increase in cancer risk.

EARLY SOVIET DESIGNED REACTORS

The April 1986 disaster at the Chernobyl nuclear power plant in Ukraine was the result of major design deficiencies in the RBMK type of reactor, the violation of operating procedures and the absence of a safety culture. One peculiar feature of the RBMK design was that coolant failure could lead to a strong increase in power output from the fission process, i.e. positive void coefficient. This was not the prime cause of the accident, however. It vindicated once and for all the desirability of designing with inherent safety supplemented by robust secondary safety provisions. By way of contrast to western safety engineering, the Chernobyl reactor did not have a containment structure like that used in the West or in post1980 Soviet designs.

The accident destroyed the reactor, and its burning contents dispersed radionuclides far and wide. This tragically meant that the results were severe, with 56 people killed, 28 of whom died within weeks from radiation exposure. It also caused radiation sickness in a further 200~300 staff and firefighters, and contaminated large areas of Belarus, Ukraine, Russia and beyond. No less than 5% of the total radioactive material in the reactor core was released from

the plant, due to the lack of any containment structure. Most of this was deposited as dust close by. Some was carried by wind over a wide neighborhood. But the problem here was not burning graphite as popularly quoted. The graphite was certainly incandescent as a result of fuel decay heat over 1000°C and some of it oxidized to carbon monoxide which burned along with the fuel cladding.

About 130,000 people received significant radiation doses, i.e. above the limits accepted by the International Commission on Radiological Protection, and continue to be monitored. About 4,000 cases of thyroid cancer in children have been linked to the accident. Most of these were curable, though about nine were fatal. No increase in leukemia or other cancers have yet shown up, but some expected. The World Health Organization is closely monitoring most of those affected.

The Chernobyl accident was a unique event and the only time in the history of commercial nuclear power that radiation related fatalities did occur. The main positive outcome of this accident for the industry was the formation of the World Association of Nuclear Operators, building on the US precedent.

The destroyed plant was enclosed in a concrete shelter which is being replaced by a more permanent structure. In retrospect, Chernobyl has not brought to light any new, previously unknown phenomena or safety issues that are not resolved or otherwise covered by current reactor safety programs for commercial power reactors. The concept of defense in depth was conspicuous by its absence, and tragically shown to be vitally important.

Apart from the RBMK design, an early Russian pressurized water reactor design, VVER440/V230, gave rise to concerns in Europe. A program was initiated to close them down as a condition for EU accession, together with Lithuania's two RBMK units.

EUROPEAN "STRESS TESTS" AND US RESPONSE FOLLOWING FUKUSHIMA

Aspects of nuclear safety highlighted by the Fukushima accident were assessed in the 143 reactors in the EU's 27 member states, as well as those in any neighboring states that decided to take part. These comprehensive and transparent nuclear risk and safety assessments, the so-called "stress tests," involved targeted reassessment of each reactor's safety margins in the light of extreme natural events, such as earthquakes and flooding, as well as on loss of safety functions and severe accident management following any initiating event. They were conducted from June 2011 to April 2012.

They mobilized considerable expertise in different countries with 500 man-years under the responsibility of each national Safety Authority within the framework of the European Nuclear Safety Regulators Group. The Western European Nuclear Regulators' Association proposed these in response to a call from the European Council in March 2011, and developed specifications.

In June 2011 the governments of seven non-EU countries agreed to conduct stress tests using the EU model. Armenia, Belarus, Croatia, Russia, Switzerland, Turkey and Ukraine signed a declaration that they would conduct stress tests and agreed to peer reviews of the tests by outside experts. Russia had already undertaken extensive checks.

In March 2012 the US Nuclear Regulatory Commission made orders for immediate post-Fukushima safety enhancements, likely to cost about $100 million across the whole US fleet. The first order requires the addition of equipment at all plants to help respond to the loss of all electrical power and the loss of the ultimate heat sink for cooling, as well as maintaining containment integrity. Another requires improved water level and temperature instrumentation on used fuel ponds. The third order applies only to the 33 boiling water reactor units with early containment designs, and will require reliable hardened containment vents which work under any circumstances.

The industry association, NEI, told the NRC that licensees with these Mark I and Mark II containments should have the capability to use various filtration strategies to mitigate radiological releases during severe events, and that filtration should be founded on scientific and factual analysis and should be performance based to achieve the

desired outcome. All the measures are supported by the industry association, which has also proposed setting up about six regional emergency response centers under NRC oversight with additional portable equipment.

AGING OF NUCLEAR POWER PLANTS

Several issues arise in extending the license of nuclear plants which were originally designed for 30- or 40-year operation. Systems, structures and components whose characteristics change gradually with time or use are the subject of attention. Some components simply wear out, corrode or degrade to a low level of efficiency. These need to be replaced.

Steam generators are the most prominent and expensive of these, and many have been replaced after about 30 years where the reactor otherwise has the prospect of running for 60 years. This is essentially an economic decision. Lesser components are more straightforward to replace as they age, and some may be safety related as well as economic. In CANDU reactors, pressure tube, or calandria, replacement has been undertaken on some older plants, after some 30 years of operation.

A second issue is that of obsolescence. For instance, older reactors have analog instrument and control systems, and a question must be faced regarding whether these are replaced with digital in a major midlife overhaul, or simply maintained.

Thirdly, the properties of materials may degrade with age, particularly with heat and neutron irradiation. In some early Russian pressurized water reactors, the pressure vessel is relatively narrow and is thus subject to greater neutron bombardment that a wider one. This raises questions of embrittlement, and has had to be checked carefully before extending licenses.

Periodic safety reviews are undertaken on most older plants in line with the IAEA safety convention and WANO's safety culture principles to ensure that safety margins are maintained. The IAEA undertakes Safety Aspects of Long Term Operation evaluations on request from member countries. These missions check on both physical and organizational aspects, and function as an international peer review of the national regulator.

SAFETY RELATIVE TO OTHER ENERGY SOURCES

Loads of occupational accident statistics have been generated over the last 40 years of nuclear power operations worldwide. These can be compared with those from coal-fired power generation. All show that nuclear is a distinctly safer way to produce electricity.

Coal-fired power generation has chronic, rather than acute, safety implications for public health. It also has profound safety implications for the mining of coal, with thousands of workers killed each year in coal mines. A major reason for coal's unfavorable showing is the huge amount which must be mined and transported to supply even a single large power station. Mining and multiple handling of so much material of any kind involves hazards, and these are reflected in the statistics.

Hydro power generation has a record of few but very major events causing thousands of deaths. In 1975 when the Banqiao, Shimantan & other dams collapsed in Henan, China, at least 30,000 people were killed immediately and some 230,000 overall, with 18 GWe lost. In 1979 and 1980 in India some 3,500 were killed by two hydroelectric dam failures. In 2009 in Russia 75 were killed by a hydro power plant turbine disintegration.

In the UK, Friends of the Earth commissioned a study by the Tyndall Center, which drew primarily on peer-reviewed academic literature, supplemented by literature from credible government, consultancy and policy sources. It concluded in January 2013 that the safety risks associated with nuclear power appear to be more in line with life cycle impacts from renewable energy technologies, and significantly lower than for coal and natural gas per MWh of supplied energy.

ADVANCED REACTOR DESIGNS

The designs for nuclear plants being developed for implementation in coming decades contain numerous safety improvements based on operational experience. One major feature they have in common beyond safety engineering already standard in western reactors is passive safety systems, requiring no operator intervention in the event of a major malfunction.

The main metric used to assess reactor safety is the likelihood of the core melting due to loss of coolant. These new designs are one or two orders of magnitude less likely than older ones to suffer a core melt accident, but the significance of that is more for the owner and operator than the neighbors, who as TMI and Fukushima showed are safe also with older types.

REFERENCES

1. Fifth Assessment Report, IPCC (2013-2015) http://www.ipcc.ch/pdf/assessment-report/ar5/wg1/WG1AR5_ALL_FINAL.pdf
2. Energy Technology Perspectives 2014, IEA http://www.iea.org/publications/freepublications/publication/EnergyTechnologyPerspectives_ES.pdf
3. http://www.world-nuclear.org/info/safety-and-security/safety-of-plants/safety-of-nuclear-power-reactors/

International Conference on Mechanical Engineering 2015
(ICME 2015) 18 – 20 December, 2015, Dhaka, Bangladesh

Paper ID : K-03

The Research and Development of Circulating Fluidized Bed Combustion in China

Yue Guangxi

Thermal Engineering Department, Tsinghua University, Beijing 100084 China

Tel: +86-10-62792647, Fax: +86-10-62781743

Corresponding author: arupjyoti.bhowal@heritageit.edu

Abstract. CFB combustion technology is one of the effective and economical approaches for the conversion of low grade coal and coal washing waste into energy. In the past 30years, Chinese scientists and engineers have been making great efforts on the investigation CFB combustion theory and developing advanced CFB boiler to meet the need of Chinese market. Present presentation gives an introduction about the new understanding on CFB combustion theory includes two phase flow in CFB, heat transfer distribution in furnace and combustion heat distribution in furnace, besides fluidization regimes in CFB boiler. Based on these new understanding, Chinese engineers developed series capacities of CFB boilers. The update result is the success of 600MWe supercritical CFB boiler. Another practice is the low bed inventory CFB process that is forming advanced CFB boilers with lower fan power and higher availability.

BACKGROUND

So far, the major energy resource in China has been coal and this saturation can't change in the near future. While, China is facing a tough challenge to avoid pollution as burning enormous coal. Besides, it is noticed that the average ash content and sulfur content of Chinese coal are quite high. CFB combustion technology is the best solution for lower quality coal combustion and economical solution to control SOx and NOx emission. Therefore, CFB combustion technology is quite hot in China to deal with such low grade solid fossil fuel including the coal washing waste. Generally, the coal washing process products waste with 20% of raw coal in China [1]. By 2014, the capacity of CFB-based power was around 12% of China's total coal-fired power capacity.

China started his R&D on bubbling bed boiler since 1960s. By 1980, the number of operating bubbling bed boilers in China was already around 3000 [2].

Chinese started their investigation on CFB combustion as they noticed the success of the CFB demonstration boiler in Germany in 1984.

From 80's, Chinese developers spent 10 years to realize that the fluidization regimes of bubbling bed and circulating fluidized bed were different [3-8].

After 1990, China, step by step, realized the importance of CFB combustion theory and the universal poor understanding on it. They made big effort to improve the design theory of CFB boiler and finalized their own understanding on the CFB combustion theory [9, 10].

THE CONTRIBUTION ON CFB COMBUSTION THEORY BY CHINA

Two Phase Flow in a CFB Boiler

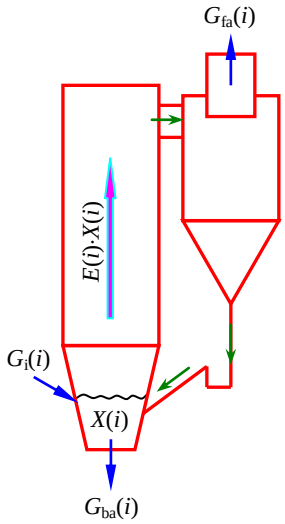

FIGURE 1. Multi size particles open system for the CFB boiler.

It is well known that CFB combustion technology was introduced from heterogenerious circulating fluidized bed reactor in chemical engineering. Chemical scientists already well defined fluidization regimes in a riser by characters of particles and fluidization gas. While, most observation on chemical reactor is based on a fact that the bed inventory in circulating fluidized bed reactor does not loss and keeps constant. This means such particle circulating loop is a closed loop. Chinese scientists realized this was not the case for coal fired CFB boiler. If we neglect the burning coal (only about couple percentages in bed inventory) in a CFB boiler, the main component of circulating particles in CFB boiler is ash. CFB boiler continually receives ash and limestone particles with wide range size and continually outputs bed ash and fly ash out of circulating loop. So that it is a multi size particles open circulating loop, but not a single size particles close circulating loop as CFB chemical reactor [11].

As shown in Fig. 1, the material balance of open circulating loop can be analyzed. Assume the fraction of size *i* particles in bed inventory is $X(i)$, the input of size *i* particle flow rate is $G_{in}(i)$. The drain flow rate of bed ash with size I particle is $G_{ba}(i)$ and the flow rate of fly ash with size I particles is $G_{fa}(i)$. Then we have:

$$G_{in}(i) = G_{ba}(i) + G_{fa}(i) \tag{1}$$

If we take the elutriation flow of *i* size particles as:

$$E(i)\cdot X(i) \tag{2}$$

We can define the cyclone fractional efficiency for *i* size particles as :

$$\eta_{fa,i} = 1 - \frac{G_{fa}(i)}{E(i)\cdot X(i)} \tag{3}$$

Bed ashes drain efficiency:

$$\eta_{ba,i} = 1 - \frac{G_{ba}(i)}{E(i)\cdot X(i)} \tag{4}$$

Open loop accumulation efficiency:

$$\eta_i = 1 - \frac{G_{fa}(i) + G_{ba}(i)}{E(i)\cdot X(i)} = \eta_{fa,i} + \eta_{ba,i} - 1 \tag{5}$$

The accumulation efficiency for open loop system of CFB boiler is shown in Fig. 2 [9].

Clearly, the fractional efficiency of CFB circulating loop is a cap shape curve that particle size corresponding highest efficiency is around 150 to 250□m. The resources of bed inventory should be also taken into account as we analyze the material balance of CFB boiler. The formation of ash particles in CFB experiences series process:

- Primary fragmentation of coal as soon as coal particles enter furnace.
- Char combustion fragmentation
- Intrinsic ash formations.
- Ash particles fast attrition period.

- Particle slow and stable attrition period.

The attrition rate of ash is strongly related with ash mineral composition; Ca content makes major contribution on the increasing of attrition rate [12].

A standard lab test procedure was set up in China to measure the ash (size) formation character and attrition rate to determine the ash input into a coal fire FB boiler [13].

Then a 1-D fluidization model for CFB furnace was built to predict the material balance and bulk density distribution in furnace [14]. The model includes:

- Open loop accumulation efficiency for different size particles sub-model.
- Particle elutriation and entrainment sub-model.
- Particle attrition rate and resident time sub-model.
- Segregation sub-model.

The coal ash formation and attrition character data were from the lab. Test.

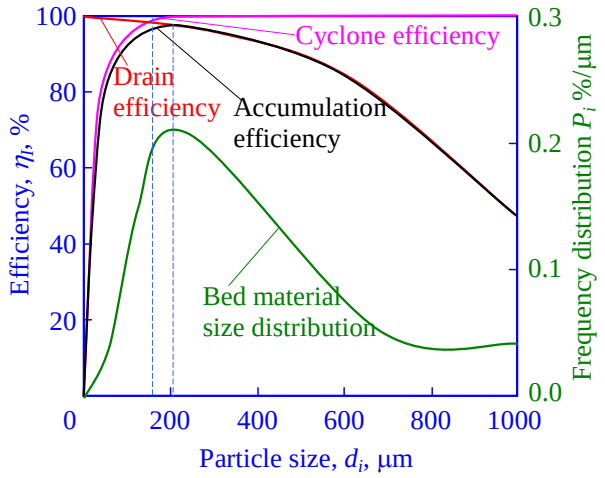

FIGURE 2. Fractional accumulation efficiency of the CFB boiler

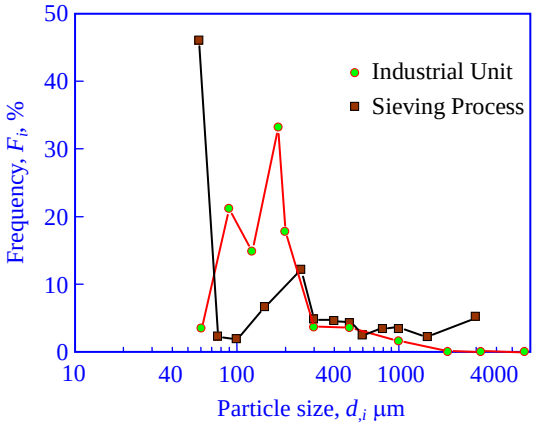

FIGURE 3. Comparison of the ash formation character between the lab. test and the field test without attrition

The prediction was validated by 3 boilers field tests and approved by Gardanne 250MWe CFB. The comparison of model prediction and field test for Gardanne CFB is interesting [14]. Fig.3 shows the difference of ash formation character by Lab. test and sampling from Gardanne CFB boiler. We could find the good agreement between them for fine and coarse particles, but big difference on particles with size 100 to 300 m. Because such size particles are the major component of bed inventory, the resident time for them is much longer than other size particles. Then the attrition of these particles should be taken into account for final ash formation in CFB boiler. Then, the attrition rate was measured and the residence time also inputted in the 1-dimension model. The new prediction agrees well with the field test, shown in Fig.4 and 5.

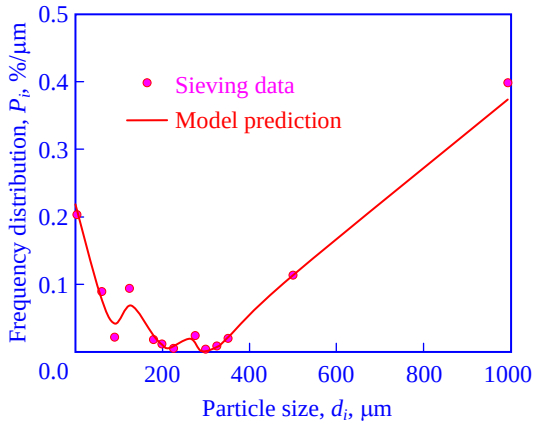

FIGURE 4. Comparison of the ash formation character between the lab. test and the field test with attrition

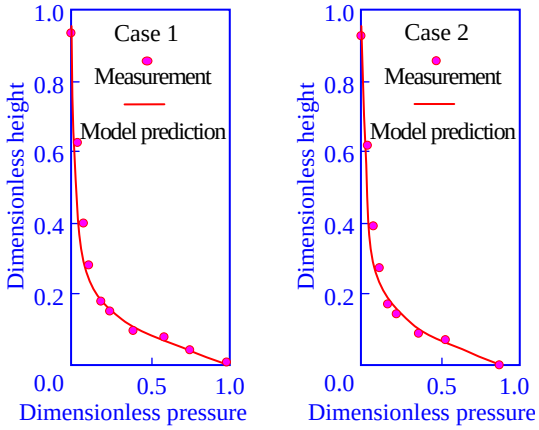

FIGURE 5. Comparison of model prediction on the pressure drop along the height of furnace with that measured in a 250MW CFB.

It is interesting for gadanne case that the attrition rate of coal ash is extremely high. The ash composition analysis proved that higher attrition rate of Gadanne coal ash is attributed to the high Ca content [13], as shown in Fig. 6.

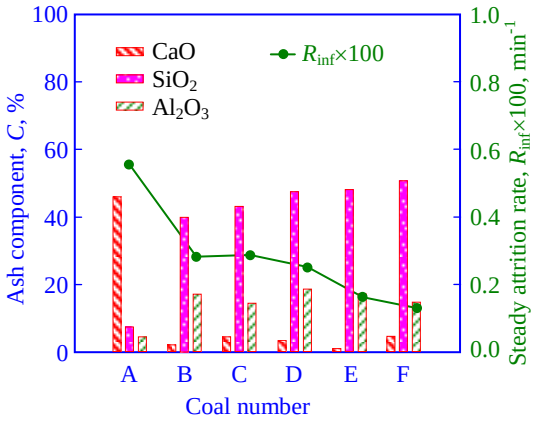

FIGURE 6. Attrition rate VS ash composition.

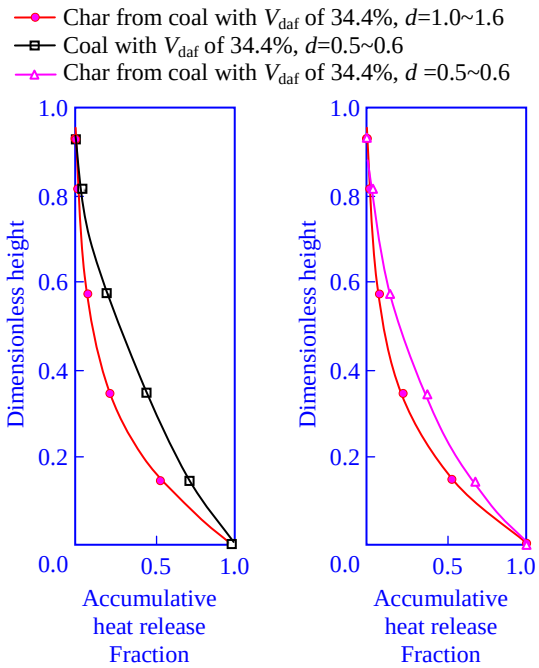

FIGURE 7. Heat releasing along the height of furnace VS coal type and size.

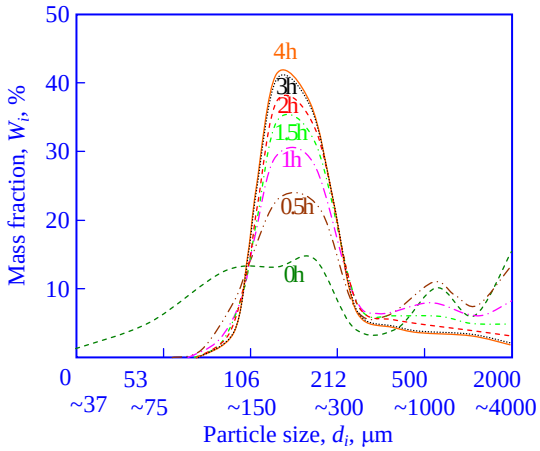

FIGURE 8 Circulation system is accumulating fine particles in CFB boiler

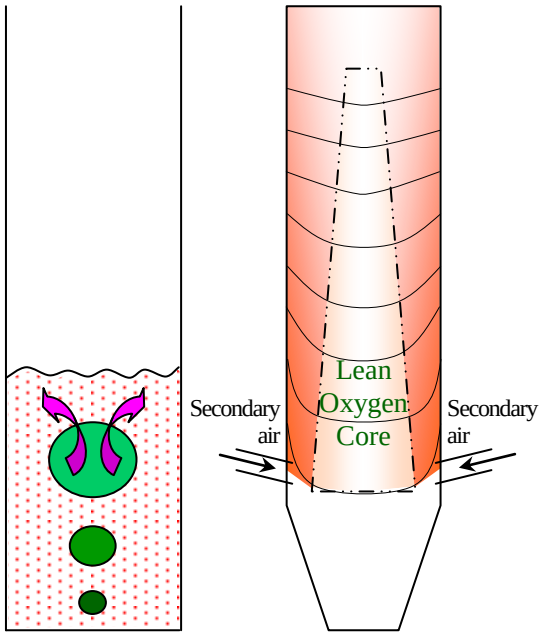

FIGURE 9 Lean condition in densebed and in the core region above second air port

Coal combustion in a CFB boiler

The coal particle combustion process in fluidized bed condition was already well investigated before. But engineers were much more care the combustion behavior of the continuing coal flow in CFB but not single coal combustion behavior. So that Chinese scientists suggested a concept as fractional heat releasing distribution along the height of furnace to describe such behavior [15]. Besides, they developed a test method to experimentally determine the 1-D distribution of heat releasing in CFB furnace or in test rig by measuring the Oxygen concentration distribution. Corresponding modeling work was also done to understand the mechanism of combustion heat releasing in CFB furnace.

It was concluded from the investigation that The heat releasing distribution is the function of fluidization status (superficial velocity and bed quality), the coal type (volatile /fix carbon ratio), coal size distribution [15], as shown in Fig. 7.

The information of heat releasing distribution is the base for the engineer to determine the P/S air ratio and the size distribution of feeding coal for CFB boiler.

Chinese researchers found the former modeling of heat releasing in CFB furnace always predicted heat released in dense bed of CFB much larger than that of field test. Carefully investigation on the behavior of fluidization status in dense bed proved the dense bed in CFB boiler is different with bubbling bed boiler on the average size of bed inventory [16]. For CFB boiler, the circulating system accumulate narrow size cut fine particle [17], as shown in Fig. 8, until the amount of such fine particle are enough to support the setting up of a fast bed at upper part of furnace. Consequently, the average size of CFB dens bed is from 1-2mm that is the average size of the inert bed material, towards 100-200μm. So that the amount of air to fluidize emulsion phase sharply decreases as average size of bed inventory decreases. Considering the carbon particle combustion in dense bed is mostly happening in emulsion phase then, the amount of air joining carbon particle combustion is not enough. Big portion of primary air is short cutting through bubble phase and never join the combustion. So we can say the carbon combustion in dense bed zone of CFB boiler is always in lean condition if the circulating system of CFB boiler works well. This analysis was matching with the experimental observation by Prof. Leckner as he found the strong fluctuation of O_2, CO concentration above the surface of dense bed in his CFB boiler [7]. The lean combustion in dense bed also limits the fractional heat releasing in dense bed zone [16].

Chinese researchers also observed the existence of a lean combustion core at the center of upper part of CFB furnace [7], as shown in Fig. 9. This is coursed by weak penetration of second air and poor horizontal mixing in fast bed. This also reminds the design engineer should take the momentum into account as he designs the speed of second air. Besides the bulk density should also be limited as design the fast bed status for a CFB boiler.

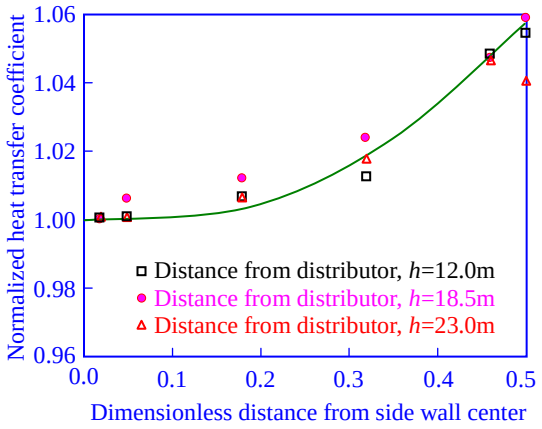

FIGURE 10 Heat flux distribution along horizontal direction in a CFB furnace

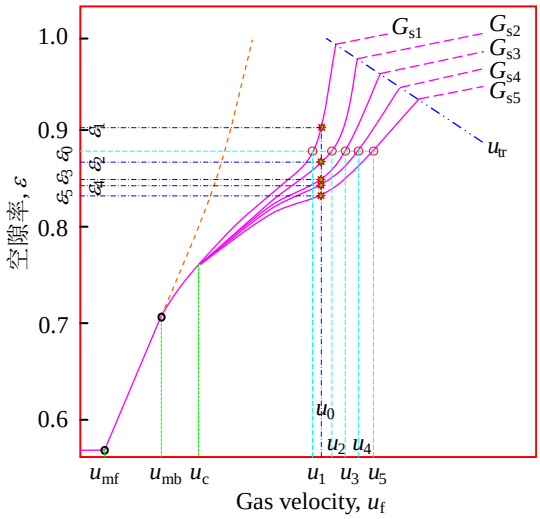

FIGURE 11 Multi status in fast bed regime.

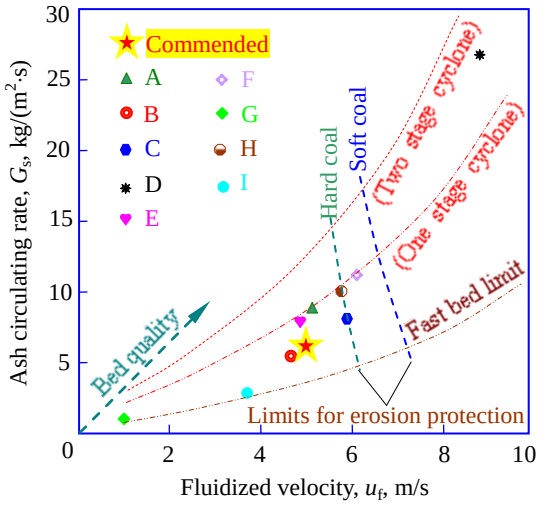

FIGURE 12 Fluidization status map of CFB boiler.

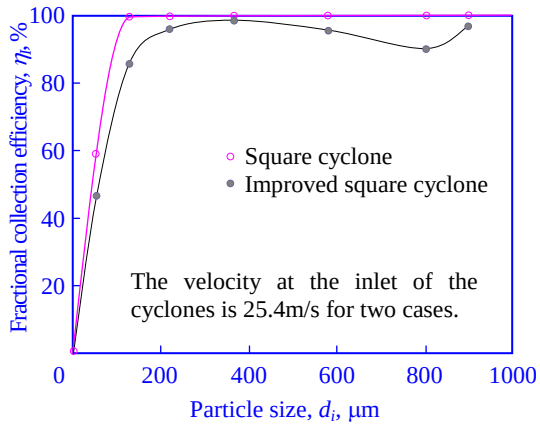

FIGURE 13 Comparison of Separator Efficiency between Improved Separator and Original One.

FIGURE 14 75t/h CFB boiler with improved square cyclone

Heat Transfer in A CFB Boiler

The mechanisms of heat transfer between water wall and combustion side were well realized by former researchers in the world that were distinguished as gas convection, particles conversion and particles radiation [5, 6]. The contribution of Chinese researchers was the comprehensive field tests to determine the semi-empirical heat transfer coefficient equation for engineering design [18]. The heat transfer mechanisms was simplified as two items: particle convection and particle radiation. They also developed local bulk density probe and heat flux probe for field tests [5]. Series tests were conducted at CFB boilers. The capacity of tested boilers covered 15MW to 300MW [5, 19, 20].. The equation they got can give a prediction of local heat transfer coefficient VS. local bulk density and furnace temperature. The accuracy of equation is satisfied for engineering design [18]. Besides, this equation is universal suitable for different CFB technologies if engineers know the bulk density distribution in furnace. One of the update progresses on the investigation of heat transfer in China was the field test for heat transfer coefficient or heat flux horizontal distribution in a 300MW CFB furnace [20]. The width of this furnace water wall is 28m. This is almost same as 600MW supercritical CFB in China. The test result is shown in Fig. 10. We noticed the heat flux at the corner of furnace was higher than the center of water wall around 5%. This fact was just conflict with the modeling prediction. And the test result is useful for the development of supercritical CFB for safety evaluation of water membrane.

Fluidization Regimes in CFB Boiler

Chinese researchers realized a CFB boiler starting process is accompanied with the accumulating of fine particles in bed inventory, until the fluidization regime in boiler from coarse particle bubbling bed to a combined bubbling bed at bottom with a fast bed at upper.

They also realized even in the fast bad regime, there can be different status corresponding to different fluidization gas speed uf and different solid carrier Gs. Although the multi status of fast bed was proved by Prof. Kwak many years ago as shown in Fig. 11, Chinese researchers expressed such multi status in fast bed regime for CFB boiler with another way [9] as shown in Fig.12.

In this map, the brown line is the distinguish line between bubbling bed and fast bed regimes. The two red lines are the limitation of Gs for one cyclone and two series cyclones CFB. The green dot line and blue dot line represent the limitation of water wall erosion. Then the fluidization status of all CFB technologies should be within a tri-angle area above the bubbling bed limitation line and under cyclone accumulation ability line. In this map, the fast bed status of all CFB technologies was marked. Clearly, some technologies already reached erosion line for hard ash coal. This fact was already proved by operating practice of such technologies in China. There are still some uncertainties for this map especially for the accuracy of Gs- ash circulating rate. While by this map, it made sense for engineers to pre-select right fast bed status as the starting point to design a CFB boiler for specific coal. After the fast bed status (Gs and uf) are determined, the material balance prediction can be done to determine the selection of

separator, loop seal size. Then, according to heat releasing character in CFB, the Primary air to secondary air ratio and size distribution of feeding coal can be confirmed. Finally the heat transfer equation offers the tool to design the heating surface for this boiler [9].

THE APPLICATION OF THE DESIGN THEORY

The development of Chinese CFB combustion technology was matching with the progress of the understanding on CFB combustion theory.

FIGURE 15 130t/h CFB boiler with improved square cyclone.

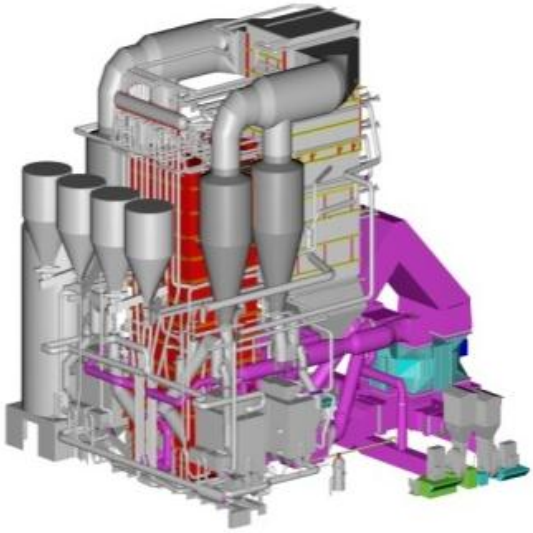

FIGURE 16 Alstom 300MW subcritical CFB boiler

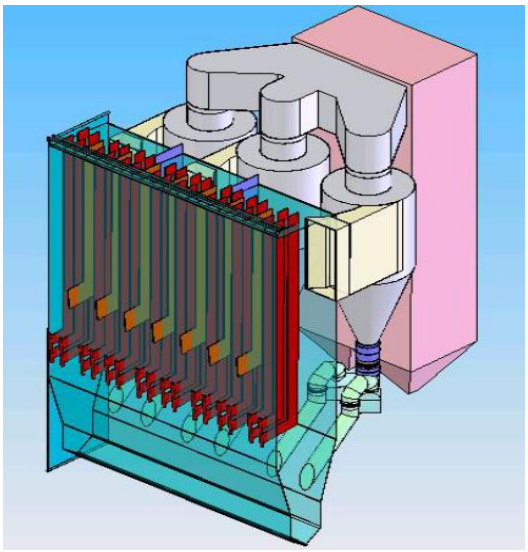

FIGURE 17 Dongfang 300MW subcritical CFB boiler

Industrial CFB boiler

From 1984 Chinese scientists spent 10 years to understand the principle of material balance in CFB boiler. They realized that the CFB circulating system should be able to accumulate enough fine particles to convert the fluidization regime from bubbling bed into fast bed. That means the d99 of the separator in CFB is somehow, even more important than d50 for the conversion of fluidization status. Fortunately, the investigation proved d99 of improved square cyclone was almost same as that of round cyclone [21], as shown in Fig. 13. So that they gave up the so called two-dimension flow type separators and adopted improved square shape cyclone separator for none reheat CFB boiler with the capacity of 75-220t/h [22, 23], shown in Fig.14, 15.

The performance of such boilers with square cyclone was much better than that with two dimension flow separator. At least, they could reach full load operation besides the structure of the boiler still kept compact. Also, as they defined the fluidization status, they re-located the fast bed status under the guidance of the fluidization map to avoid serious erosion on water wall. The reliability of these boilers was improved.

Utility CFB boiler

By 2000, the power market in China pushed the development of utility CFB boiler. Chinese boiler works licensed foreign CFB technologies to meet the market needs, like EVT, former ABB-CE, Alstom. However, the first operating experience of these technologies proved the performance was not satisfied as expected when burning Chinese coal. It looks like these technologies were developed base on limited coal types. So that boiler engineers turned to Chinese CFB design theory and guidance.

A typical example is the 300MW sub critical CFB boiler developed by Dongfang Boiler cooperated with Tsinghua University [24]. Before this boiler, the Alstom sub critical 300MW CFB was already in commercial operation, as shown in Fig. 16. Dongfang boiler considered the complex structure and the hard maintenance besides the higher auxiliary power consumption of Alstom CFB boiler, and then they accepted the idea from Tsinghua. The key points of new design were re-specified the fast bed status in furnace to avoid erosion; accepted new material balance model and heat transfer equation. The flow pattern in furnace was evaluated by a cold model test in Tsinghua University. According to the comments from Tsinghua, the boiler accepted the in furnace wing wall instead of external heat exchanger. The pants leg furnace also gave up. The cyclone was scaling up so as to decrease the number of them. Then the overall structure of the boiler became M Type instead of original H type. It became much simpler, as shown in Fig.17. The operating performance of new CFB boiler was so satisfied by Chinese clients, that Dongfang Boiler quickly dominated Chinese subcritical 300MW CFB market. This even pushed other Chinese giant boiler works to develop similar 300MW CFB [25].

600MW supercritical CFB boiler

China started the investigation of supercritical CFB since 2000. At that time, there were only few literatures mentioned about the possibility to develop SC CFB. Chinese scientists were facing big challenges for this dream. The major risks were:

- The scaling up of the furnace and corresponding knowhow about two phase flow, mixing, combustion and heat transfer in larger furnace.
- The risk as combining force circulation in water side with unknown heat flux distribution in combustion side of CFB.
- The unknown dynamic behavior of supercritical water forced circulating as combined with large inertia CFB process.

Started by a PhD. thesis to prove the technical possibility of SC CFB in 2000 [26], Chinese MOST (Ministry of Science and Technology of PRC) first funded a project to investigate the key technologies related to the development of SC CFB boiler in 2003. In 2005, Chinese.

NDRC (National Development and Reform Commission) and MOST both issued the programs to develop the demonstration of 600MW SU CFB. A big R&D team was forming since then, including research institutes, boiler works and potential clients. By 2011, the engineering project was approved by NDRC. The demonstration of 600MW SC CFB power plant was erecting in 2012-2013. By the April of 2013, the power plant passed 168 hours full load operation test, and handed over to client for commercial operation. Fig. 17 is the picture of operating 600MW SC CFB power plant. The performance test of the demonstration proves the major parameters of the boiler are well agreed with the design value. The emission data is even better than design. The detail of this demonstration is introduced by another paper in present conference [27].

FIGURE 18 .The picture of operating 600MW SC CFB power plant.

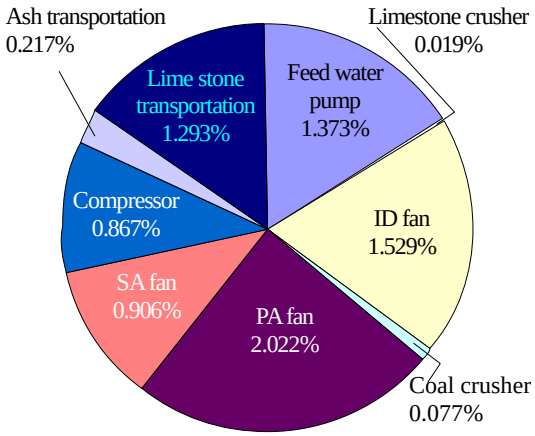

Auxiliary power total 8.303%

FIGURE 19 .Auxiliary power consumption for a 300MW CFB

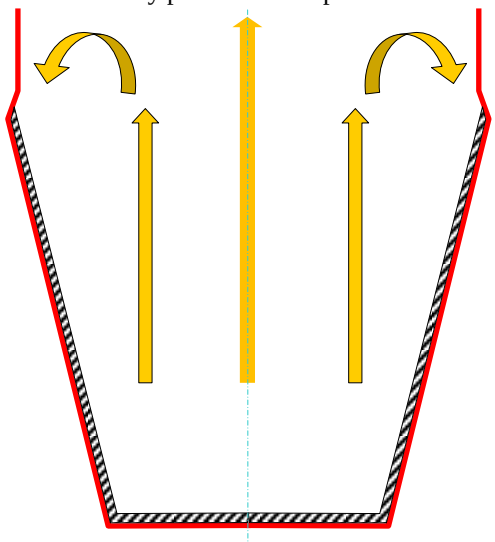

FIGURE 20 . Erosion occurring on water wall in CFB furnace

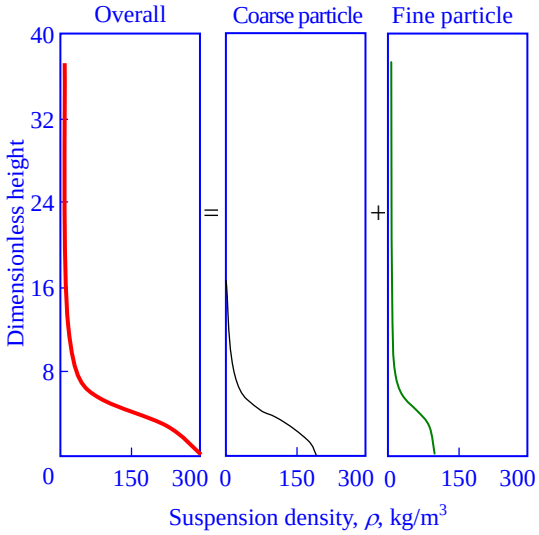

FIGURE 21 The combination of fast bed and bubbling bed in CFB furnace

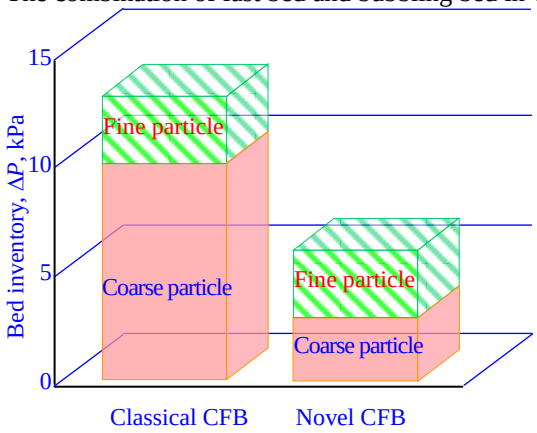

FIGURE 22 Classification of bed inventory.

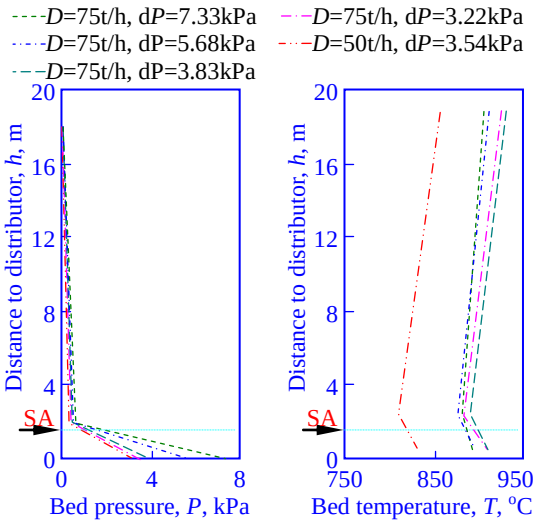

FIGURE 23 Pressure and temperature profiles for CFB at low bed inventory operating.

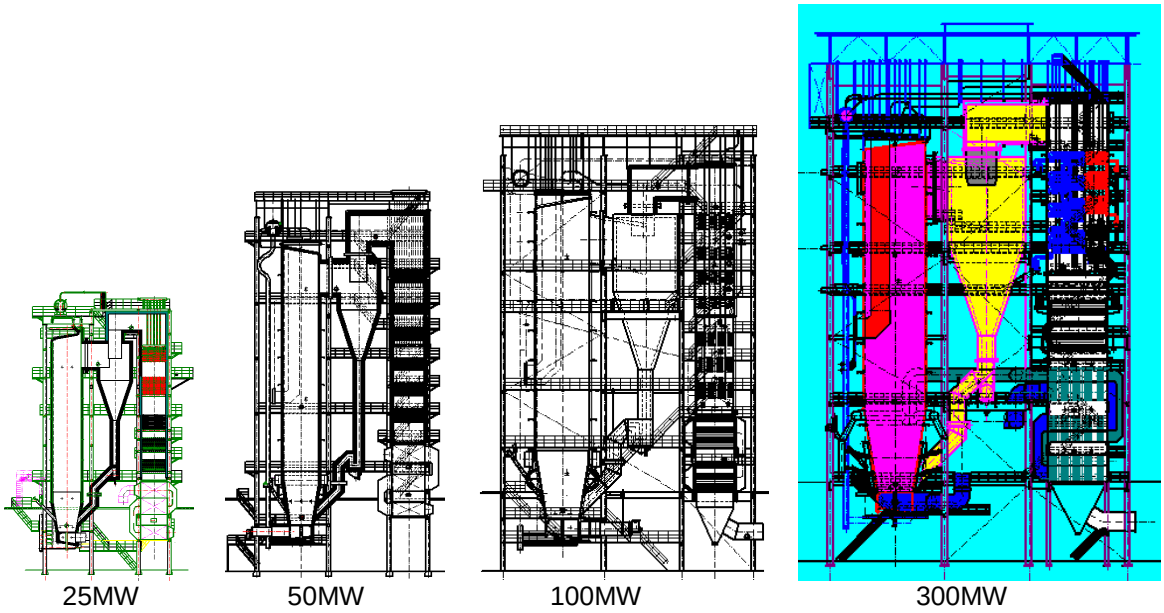

FIGURE 24 Series capacity of low bed inventory CFB boilers

Now, the other two 600 MW SC CFB boilers are under constructing. And based on the experience of the 600 MW SC CFB boiler, the 350MW SC CFB boiler was developed. The ordered 350 SC CFB boilers exceeds 20. Most of them are erecting.

Low bed inventory CFB boiler

Although CFB combustion is entering utility market, there are still two defects compared with pulverized coal (PC) combustion technology:

- 8-12 kPa bed inventory needs higher pressure head of draft fan. The average auxiliary power of CFB is 2-3% higher than PC, shown in Fig. 19.
- Enormous ash circulating flow causes serious erosion at inter-section between bottom refractory line and vertical water wall, shown in Fig.20. This erosion has big impact on the availability of CFB power plant.

Chinese scientists investigated the possibility to decrease the bed inventory so as to bate the erosion and fan power. In fact, bed inventory can be divided as two kinds of particles [28]. Large particles stay in dense bed. Small particles can be entrained by flue gas and forming fast bed above dense bed, shown in Fig.21.

The amount of fine particle should be more than a limitation that creates fast bed status. The amount of coarse particles should guarantee enough resident time for large coal particle burn out. As shown in Fig.22, if we try to decrease the total bed inventory, the only way is to improve the bed quality so as to keep enough fine particles forming fast bed. Two measures were taken for the improvement of bed quality:

- Decreasing the fraction of coarse particle in feeding coal.
- Improving the performance of circulating loop of CFB include cyclone efficiency and loop seal.

In 2007, the first demonstration of low bed inventory CFB boiler with capacity 75T/h was in operating. It showed the bed inventory could be ranging 3220-7330 Pa without big variation of temperature [29], as shown in Fig. 23.

Then the low bed inventory CFB technology quickly entered in market and forming series capacity products as shown in Fig. 24.

More than hundreds of low bed inventory CFB boilers were in operation. Average fan power saving was 30%, erosion sharply decreasing. Then the availability of them reached over 6000h/year. Even average boiler efficiency was improved 1%.

The 350MW SC CFB boiler with Low bed inventory is being designed. And Low bed inventory CFB technology will be adopted in the future demonstration of 660MW USC CFB boiler.

REMARK

CFB technology is the best choice for the utilization of large amount of low grade coal and coal washing waste in China.

Chinese researchers and engineers are making big effort to investigate CFB combustion theory and made their contribution.

Chinese engineer have been practicing the design theory in the development of CFB. They spent 30 years to develop series capacities CFB boiler until the update 600MW supercritical CFB demonstration.

At same time, they investigated the low bed inventory CFB process and commercialized it. The new CFB saves 30% fan power and improves the availability of operation.

ACKNOWLEDGEMENT

Financial support of this work by Key Project of the National Twelve-Five Year Research Program of China (2012BAA02B01) and the National Basic Research Program of China (973 Program) (2014CB744305) and MOST Program 2011DFA60390 are gratefully acknowledged.

REFERENCE

1. Wang Q, Feng Y, Lu J, et al. Numerical study of particle segregation in a coal beneficiation fluidized bed by a TFM-DEM hybrid model: Influence of coal particle size and density. Chemical Engineering Journal, 2015, 260: 240-257.
2. Lu J, Wu E. The status and future of domestic circulating fluidized bed boiler. Proceedings of 1993' Academic Meeting of Chinese Electricity Institute, Heat and Electricity Branch, Guilin, 1993: 152-159.
3. Lu J, Jin X, Yue G, Zhang J, et al. Hot test of material balance in a 75t/h CFB boiler with water cooled square separator. Journal of Tsinghua University, 1998, 38(5): 7-10.
4. Yang H, Bob Mchugh, Lu J, et al. The Effect of particle size distribution on pressure profile in cfb riser. In: Xu X C ed. Proceedings of the 4th Int. Symp. on Coal Combustion, Beijing, 1999: 459-464.
5. Jin X, Lu J, Li Y, et al. Experimental investigation on heat transfer in industrial-scale circulating fluidized bed boilers. In: Werther J ed. Proceedings of the 6th International Conference of CFBC, Weirsberg, 1999: 356-361.
6. Zhang J, Lu J, Yang H, et al. Investigation on heat transfer in CFB boilers. In: Xu X C ed. Proceedings of the 4th Int. Symp. on Coal Combustion, Beijing, 1999: 436-442.
7. Lu J, Jin X, Yue G, et al. Gas concentration profiles in the furnace of large CFB boilers with water-cooled square separator. In: Tian Changlin, Cai Ruixian, Xu Jianzhong eds. Proceeding of the First International Conference of Engineering Thermalphysics, Beijing, 1999: 610-615.
8. Ma L, Lu J. Primary Fragmentation behavior of coal in a fluidized bed combustor. In: Xu X C ed. Proceedings of 4th International Symposium of Coal Combustion. Beijing, 1999: 506-513.
9. Yue G, Lu J, Zhang H, et al. Design theory of circulating fluidized bed boilers. In: Lufei Jia ed. Proceeding of the 18th International Conference on Fluidized Bed Combustion. Toronto: ASME, 2005: 135-146.
10. Yang Hairui, Lu Junfu, Yue Guangxi. Design theory of a circulating fluidized bed boiler and the measurement of the fuel property. Power Engineering, 2006, 26(1): 42-48.
11. Lu J, Feng J. On design of CFBC boilers. In: Xuchang Xu ed. Proceeding of the 5th International Symposium on Coal Combustion, Nanjing China, 2003: 309-313.
12. Wang J, Zhao X, Li S, et al. Influence of coal ash components on attrition characteristics in circulating fluidized bed. Journal fo Chemical Industry and Engineering, 2007, 58(3): 739-744.
13. Yang H, M Wirsum, Lu J, et al. Semi-empirical technique for predicting ash size distribution in CFB boilers. Fuel Process Technology, 2004, 85(12): 1403-1414.
14. Yang H, Yue G, Xiao X, et al. 1D modeling on the material balance in CFB boiler. Chemical Engineering Science, 2005, 60(20): 5603-5611.
15. Jin X, Lu J, Qiao R, et al. Research on coal combustion fraction distribution in circulating fluidized bed combustor. Clean Coal Technology, 1999, 5(1): 20-23.
16. Jin X, Lu J, Yang H, et al. Comprehensive mathematical model for coal combustion in the circulating fluidized bed combustor. Tsinghua Science and Technology, 6(4): 319-325.

17. Lu J, Zhang J, Yang H, et al. Coal combustion efficiency in circulation fluidized bed. Journal of Basic Science and Engineering. 2000, 8(1): 97-105.
18. Lu J, Zhang J, Yue G, , et al. Heat transfer coefficient calculation method of the heater in the circulating fluidized bed furnace. Heat Transfer - Asia Research, 2002, 31(7):540-550.
19. Wang Y, Lu J, Yang H, et al. Measurement of heat transfer in a 465t/h circulating fluidized bed boiler. In: Lufei Jia ed. Proceeding of the 18th International Conference on Fluidized Bed Combustion. Toronto: ASME, 2005: 327-335.
20. Zhang P, Lu J, Yang H, et al. Heat transfer coefficient distribution in the furnace of a 300MWe CFB boiler. In: Yue G, Zhang H, Zhao C, et al. eds. Proceedings of the 20th International Conference on Fluidized Bed Combustion. Xi'an, Beijing: Springer Press. 2009: 167-171.
21. Yue G, Li Y, Liu Q, et al. The first pilot compact CFB boiler with water cooled separator in China. In: Large J F ed. Proceedings of the 14th International Conference on Fluidized Bed Combustion, Wancouwer, 1997: 497-506.
22. Lu J, Yue G, Liu Q, et al. Operation experience of a 130t/h circulating fluidized bed boiler with water cooled square cyclone. Chinese Electric Power, 2001, 34(10): 19-23.
23. Lu J, Liu Q, Zhang J, et al. The design and operation experience of the first pilot 220t/h circulating fluidized bed boiler with water cooled square cyclone. Proceedings of the CSEE, 2003, 23(8): 178-182.
24. Yue G, Yang H, Nie L, et al. Hydrodynamics of 300MWe and 600MWe CFB boilers with asymmetric cyclone layout. In: Werther J ed. Proceedings of the 9th International Conference of CFB, Hamberg, 2008: 153-158.
25. Li J, Mi J, Hao J, et al. Operational status of 300MWe CFB boiler in China. In: Yue G, Zhang H, Zhao C, et al. eds. Proceedings of the 20th International Conference on Fluidized Bed Combustion. Xi'an, Beijing: Springer Press. 2009: 243-246.
26. Lu J. Investigation on Heat Flux and Hydrodynamics of Water Wall of a Supercritical Pressure Circulating Fluidized Bed Boiler. PhD thesis. Beijing: Tsinghua University, 2005.
27. Yue G, Ling W, Lu J, et al. Development and demonstration of the 600 MW supercritical CFB boiler in Baima power plant. Proceeding the 22th International Conference on Fluidized Bed Combustion. 2015.
28. Yang S, Yang H, Lu Jet al. The new generation combustion technology for energy saving circulating fluidized bed boilers. Journal of Power Engineering, 2009, 29(8): 728-732.
29. Yang H, Yue G. Zhang H, et al. Updated design and operation experience of CFB boilers with energy saving process in China. VGB PowerTech, 2011, 91(7): 49-53.

ICME2015

International Conference on Mechanical Engineering 2015
(ICME 2015) 18 – 20 December, 2015, Dhaka, Bangladesh

Paper ID : K-04

Heat Transfer in Completely and Partially Filled Spherical Phase Change Thermal Energy Storage Modules

Muhammad Mustafizur Rahman[a)]

Department of Mechanical Engineering, Wichita State University, Wichita, Kansas 67260-0133, USA

[a)]Corresponding author: muhammad.rahman@wichita.edu

Abstract. A comprehensive investigation of heat transfer and induced fluid flow interactions during melting in a confined storage medium is reported in this paper. This study focuses on thermal characterization of a single constituent storage module rather than an entire storage system to precisely capture the energy exchange contributions of all fundamental heat transfer mechanisms during phase change process. Two-dimensional, axisymmetric, transient equations for mass, momentum and energy conservation were solved numerically by the finite volume scheme. Results report the influence of the Grashof, Stefan and Prandtl numbers on the melting dynamics of capsules with various diameters (20, 30, 40, and 50 mm). Also the effects of the shell material have been analyzed. Correlating equations for melt fraction and Nusselt number have been developed for possible general design applications.

INTRODUCTION

Thermal energy storage (TES) systems can be integrated in concentrated solar power plants to provide a temporal heat accumulation during the daytime operation at design conditions and use this energy for night time or low irradiation periods in order to increase the dispatch ability of the power production facility and to operate it in a cost-effective fashion. One of the heat storage approaches that has recently gained significant attention is the macro encapsulation technique for a packed bed heat exchanger, in which a large quantity of thin-walled capsules filled with a phase change material (PCM) are used as the filler material in a containment vessel through which the heat transfer fluid (HTF) is allowed to flow. During the charging mode, a fraction of the high temperature HTF coming from the solar field is pumped through the storage device and heat is transferred from the fluid to the PCM capsules and latent energy is stored in the storage material as it melts. In the discharge operation thermal energy is released from the PCM as it solidifies and heat is transferred to the HTF. Consequently, one of the main aspects in the design process of latent heat TES systems is the rate at which melting and solidification of the encapsulated storage material takes place.

A number of studies have been reported in the literature associated with melting within spherical containers. Moore and Bayazitoglu [1] numerically and experimentally investigated the melting of n-octadecane in a glass spherical enclosure. It was found that the natural convection effects can be neglected at small Stefan numbers. The mathematical model neglected the buoyancy induced flow in the liquid phase. Bahrami and Wang [2] presented an approximate closed-form solution of melting within spheres. Roy and Sengupta [3] reported an analytical solution for the melting rate at the lower surface of the solid core in a spherical capsule. The analysis was based on the technique originally developed by Bareiss and Beer [4] for cylindrical geometries. The predicted melting rate showed good agreement with the experimental data reported by Moore and Bayazitoglu [1]. Roy and Sengupta [5] analyzed the effect of natural convection during unconstrained melting with an isothermal boundary condition. Fomin and Saitoh [6] presented a numerical and analytical investigation of the melting process in a spherical capsule. The wall temperature boundary condition was specified by a sinusoidal function. The approximate analytical solutions of close-contact melting obtained by the perturbation technique were found to be in good agreement with the numerical solution.

Khodadadi and Zhang [7] demonstrated that melting in the upper part of a PCM sphere is much faster than in the lower part due to buoyancy induced convection. They also noted that conduction is predominant only during the early

part of the melting process and highlighted the use of Rayleigh number to characterize convection in this problem. Assis et al. [8] reported numerical and experimental analyses of melting in an open spherical enclosure. A combined PCM-air system was analyzed with the air space in the upper part of the shell to account for the volume expansion during the phase change process. The model took into account the density difference between the solid and liquid PCM, natural convection in the molten PCM and the air, and the vertical motion of the solid PCM. Observations from the numerical model were validated through experiments using a low melting point wax in a glass container, submerged in a water bath. The Nusselt number and melt fraction results were presented as a function of the Fourier, Stefan, and Grashof numbers.

Tan [9] reported an experimental comparison between the constrained and unconstrained melting processes of n-octadecane inside a glass container. Later, Tan et al. [10] performed numerical simulations and experiments on a vertically constrained paraffin wax sphere. They confirmed the quasi-steady behavior of the upper part of the sphere while observing the unstable melting pattern of the bottom of the sphere. In this region, a convective rising hot "jet" is reported as well as a chaotic convective behavior. The authors highlighted an underestimation of waviness at the bottom part of the sphere during experiments. They concluded that the influence of the support structure used to constrain the PCM is non-negligible. Hosseinizadeh et al. [11] reported a numerical investigation of melting of nano-enhanced phase change material in a spherical container. The effect of different nano-particle volume fractions (0, 0.02 and 0.04) on the melting rate was analyzed. The computational domain was defined similar to that developed by Assis et al. [8]. Simulation results show a melting rate enhancement of the nano-enhanced phase change materials with respect to the conventional PCM due to higher thermal conductivity. Hosseinizadeh et al. [12] presented a numerical analysis on the melting process of n-octadecane in an open spherical glass container. A uniform temperature boundary condition was imposed at the outer wall of the shell. The Computational findings were validated with the experimental results reported by Tan [9]. Good agreement was found between the numerically predicted results and the experimental data for the case where the solid phase motion was not restricted. Rizan et al. [13] reported an experimental investigation of n-octadecane melting inside a spherical shell subjected to a uniform heat flux at the outer surface of the shell. In this study, the effect of Stefan number on the melt fraction rate is highlighted.

In this study a numerical model has been developed to simulate the heat transfer and fluid dynamics that occur during the melting of sodium nitrate encapsulated in a spherical shell and subjected to a constant temperature boundary condition at the outer wall of the shell. Although this paper primarily focuses on $NaNO_3$, with a melting point of 306.8 ^oC, the proposed numerical model can be used to predict the melting process in other PCMs with different encapsulation materials and under different boundary conditions. The main differentiating aspects of this investigation with the previously reported studies include: (a) a more realistic physical representation of the encapsulated system considering a closed container, (b) the analysis of the capsule internal pressure variation due to the volumetric expansion during the phase change process, and (c) enlargement of the correlation between heat transfer and melting fraction with dimensionless numbers at relatively high melting temperatures, which can be used in future analysis during the design process of packed bed heat exchangers using encapsulated PCMs.

MODELING AND COMPUTATION

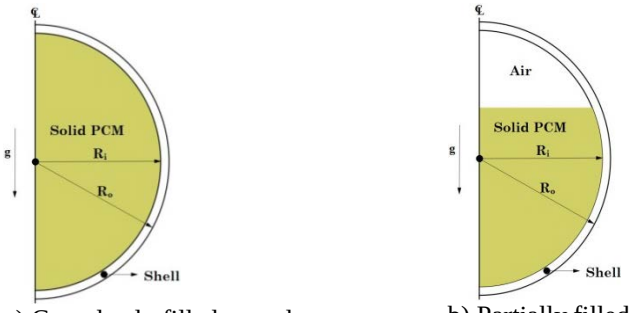

a) Completely filled capsule b) Partially filled capsule

FIGURE 1. Schematic of the analyzed configurations.

The PCM capsule is schematically shown in a cross sectional view in Figure 1. We considered both completely filled capsule where there is no residual air within the shell and the wall material is elastic and can expand or contract to accommodate for volume change with temperature and partially filled capsule where there is residual air within the

PCM capsule left during the filling progress. In the latter case, the shell material can be quite rigid such as a ceramic while the air space provides room for volumetric expansion during phase change. $NaNO_3$ has been used as the phase change material in this study. Initially the PCM is in its solid state at a temperature T_o and at time t>0, the outer boundary surface is subjected to a uniform temperature T_w which is higher than its melting temperature T_m. It may be noted that the fluid flow and heat transfer in the capsule is axisymmetric around the vertical axis of the sphere and conduction is the only mode of heat transfer through the solid shell material. The following assumptions are considered: (1) both air and liquid/solid $NaNO_3$ are homogeneous and isotropic; (2) the liquid phase is a viscous Newtonian fluid; (3) the flow is laminar and has no viscous dissipation; (4) melting of $NaNO_3$ takes place in the interval between 306.3 and 306.8 ºC where the density in the mushy zone varies linearly from 2130 kg/m^3 at 306.3 ºC to 1908 kg/m^3 at 306.8 ºC; (5) the temperature dependent PCM liquid phase density has been defined based on the expression: $\rho_{Liq} = \rho_m/\beta(T - T_m) + 1$; (6) the ideal gas equation of state is used to model the air density; and (7) no-effect associated with the gas-liquid surface tension is considered. This investigation is mainly directed to the evaluation of the melting dynamics of Sodium Nitrate, however, in order to assess the effect of the Prandtl number on the melting process, another PCM (Rubitherm GmbH, RT27) has been included for comparison purpose.

The problem has been modeled by solving the equations for the conservation of mass, momentum, and energy numerically using a control volume discretization approach [14] along with the enthalpy-porosity method [15] to track the melting front. The motion of the Air/PCM interface in the multiphase system was tracked by the Volume of Fluid (VOF) model. The model defines the volume fraction of the i^{th} fluid (α) which is defined as:

$$\alpha = \frac{volume\ of\ the\ phase\ in\ a\ cell}{volume\ of\ the\ cell} \tag{1}$$

and it takes the following values:

$$\begin{aligned} \alpha_i &= 0 \quad if\ the\ cell\ is\ empty\ of\ the\ i^{th} fluid \\ \alpha_i &= 1 \quad if\ the\ cell\ is\ full\ of\ the\ i^{th} fluid \\ 0 < \alpha_i &< 1 \quad if\ the\ cell\ contains\ the\ fluid\ interfa \end{aligned} \tag{2}$$

Based on that, the mass conservation equation is:

$$\frac{\partial}{\partial t}(\alpha_i \rho_i) + \nabla \cdot (\alpha_i \rho_i \boldsymbol{u_i}) = 0, \tag{3}$$

where $\mathbf{u_i}$ is the velocity vector of the ith fluid. The linear momentum conservation equation can be expressed as:

$$\frac{\partial}{\partial t}(\alpha_i \rho_i \boldsymbol{u_i}) + (\boldsymbol{u_i} \cdot \boldsymbol{\nabla})(\alpha_i \rho_i \boldsymbol{u_i}) = -\alpha_i \boldsymbol{\nabla} P + \alpha_i \rho_i \boldsymbol{g} + \alpha_i \mu \boldsymbol{\nabla}^2 \boldsymbol{u_i}, \tag{4}$$

Finally, the energy conservation equation can be written as:

$$\frac{\partial}{\partial t}(\alpha_i \rho_i \hbar_i) + \boldsymbol{\nabla} \cdot (\alpha_i \rho_i \boldsymbol{u_i} \hbar_i) = \alpha_i \left(\frac{\partial P}{\partial t} + \boldsymbol{u_i} \cdot \boldsymbol{\nabla} P\right) + \alpha_i \boldsymbol{\nabla} \cdot (\kappa_i \boldsymbol{\nabla} T)$$

The computational domain was discretized using a structured longitude/latitude spherical grid consisting of 10446 quadrilateral cells with marked consideration at the PCM-Air interface and mesh parameters like maximum aspect ratio and element orthogonal quality. Solution dependence on grid size and time step have been evaluated by performing calculations with different grid densities and time steps. Based on that, the time step was set to 0.004 s and 10466 cells were used for all the calculations to generate grid independent numerical results for all study cases. Convergence of the solution was checked for each time step. Scaled absolute residuals of 10^{-4}; 10^{-6} and 10^{-8} were used for the continuity, velocity components and energy equations, respectively. Commercially available software Ansys/Fluent v12 was employed for calculations. The governing equations were solved using the segregated solver. The energy and linear momentum equations were discretized using the First Order Upwind scheme. The Pressure Staggering Option (PRESTO) was used to discretize the pressure correction equation. The Semi-Implicit Method for Pressure-Linked Equations (SIMPLE) was used in the discretization process of the continuity equation (Pressure-

Velocity Coupling). The under-relaxation factors for Pressure, Momentum, and Liquid fraction were 0.3, 0.4, and 0.9, respectively. Cell kinetic and thermodynamic properties were calculated as volume-fraction-averaged of the corresponding properties of each phase, for example, density is calculated as:

$$\rho = \alpha_{air}\rho_{air} + \alpha_{pcm}\rho_{pcm} \tag{6}$$

Experimental results reported by Tan [9] have been used to validate the developed numerical model. In the experiments, the melting process of n-octadecane inside a spherical glass capsule was visualized and reported. The spherical container of 50.83mm inner radius and 1.5mm wall thickness was initially maintained 1°C below the PCM melting temperature (28°C) and, for time t>0 the outer surface of the sphere was kept at 40°C. The solid fraction evolution for both experimental and numerical results obtained from our simulations for the same problem is shown in Figure 2. The numerically predicted melt fraction rate shows good agreement when compared to the results obtained in the experiments.

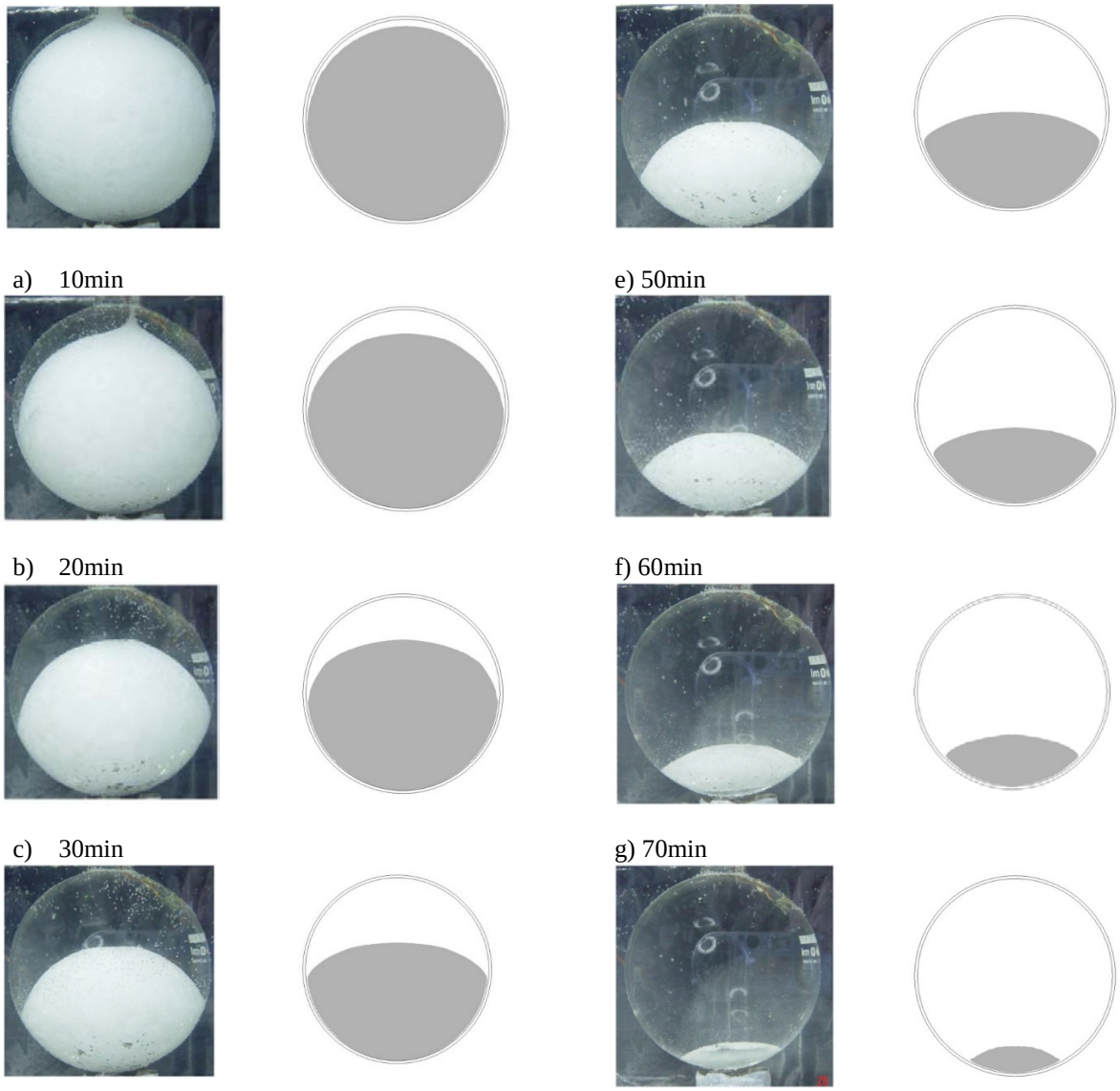

a) 10min e) 50min

b) 20min f) 60min

c) 30min g) 70min

d) 40min h) 80min

FIGURE 2. Comparison between the experimental results of Tan [9] and the numerical results of this study.

RESULTS AND DISCUSSION

For the completely filled capsule, thirteen configurations were analyzed as presented in Table 1. The effect of the outer wall temperature on the melting process for a constant capsule size is considered in cases 1 to 3. In cases 2, 4 and 5, the effect of the Stefan number is studied by keeping the Grashof number approximately unchanged. The effect of Grashof number on the melting process for a constant Stefan number, i.e. equal shell outer surface temperature (T_w= 316.8°C), is analyzed in cases 2 and 6 to 8. The effect of Prandtl number is analyzed by comparing the cases 6 and 9 for constant Stefan and Grashof numbers. Cases 7, 10 and 11 have been included in order to evaluate the influence of the shell material parameter χ ($\chi = 1 - \kappa_{pcm}/\kappa_{shell}$). The values of χ were selected for this study to lie between the limiting cases corresponding to the low and high thermal conductivity values. The selected materials are Nickel alloy, Silicon Dioxide and Zinc for cases 7, 10 and 11 respectively. In order to assess the effect of the initial temperature of the system on melting, cases 11 to 13 have been considered. A sub-cooling parameter ξ has been defined as $\xi = 1 - T_i/T_m$.

Table 1. Analyzed Study Cases.

Case number	$R_i\ (m)$	$T_w - T_m$ (°C)	Gr_R	Pr	Ste	χ	ξ
1		5	$1.32x10^4$	8.98	0.048		
2	0.010	10	$2.69x10^4$	8.90	0.097	0.966	0.00259
3		15	$4.13x10^4$	8.81	0.145		
4	0.0092	12.6	$2.68x10^4$	8.84	0.122	0.966	0.00259
5	0.011	7.5	$2.66x10^4$	8.93	0.072		
6	0.015		$9.09x10^4$				
7	0.020	10	$2.15x10^5$	8.90	0.097	0.966	0.00259
8	0.025		$4.21x10^5$				
9	0.034	9.6	$9.09x10^4$	35	0.097	0.966	0.00259
10	0.02	10	$2.15x10^5$	8.90	0.097	0.6709	0.00259
11						0.9945	
12	0.02	10	$2.15x10^5$	8.90	0.097	0.6709	0.0172
13							0.0259

The effect of the shell outer surface temperature was examined by analyzing cases 1 to 3. A 10 mm inner radii pellet was subjected to three different boundary condition values above the PCM melting temperature. The predicted liquid mass fraction for the aforementioned cases is presented in Figure 3(a). Faster melting was achieved with higher values of the shell outer wall temperature. The melting time was 33.76% shorter for Case 2 (T_w-T_m=10°C) and 48.60% shorter for Case 3 (T_w-T_m=15°C) when compared to the corresponding value of case 1 (T_w-T_m=5°C). The influence of the outer wall temperature on the heat transfer rate at the inner surface of the shell is presented in Figure 3(b). Initially, thermal energy is transferred by conduction through the shell wall due to the temperature difference between T_w and T_o, consequently high values of the heat transfer rate are observed at the beginning of the process. As the heating process proceeds, inward melting begins with the creation of the first layer of the molten PCM in the vicinity of the inner surface of the shell. The combined effect of the shell wall and molten PCM thermal resistances generates a sharp decrease in the heat transfer curves as observed during the early stages of all the curves in Figure 3(b). As the molten PCM layer gets larger, the contribution of natural convection (induced by the PCM liquid density gradient) becomes significant; consequently the value of the heat transfer rate starts to increase and subsequently reaches a maximum. After this period, all the curves present a slow decay trend with a progressive decrease toward the thermal equilibrium state of no energy transport. A similar trend has been reported and described by Sparrow et al [16]. During the time period, $0 \leq t \leq 2.2$ min, the average heat transfer rate increases with an increase of the outer wall temperature. However after this interval all the curves cross each other and an inverse trend is observed. The reason

for that is the fact that thermal equilibrium will be reached sooner for the case with the higher wall and PCM melting temperature difference (higher Stefan and Grashof numbers).

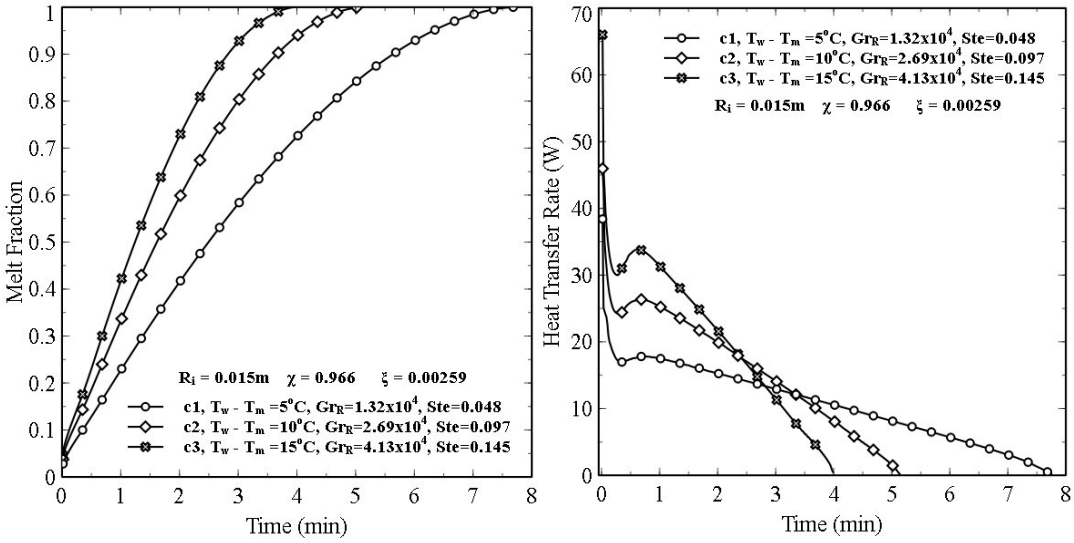

FIGURE 3. Effect of the outer wall temperature on the melt fraction and heat transfer rate.

The numerically predicted solid fraction, streamlines and isotherms contours for case 13 are presented in composite diagrams illustrated in Figure 4 at different dimensionless times. The streamline contours are shown on the right half of each circle whereas the temperature contours are drawn on the left half, with the vertical axis of the sphere separating the two fields. The solid fraction distribution at the given instant is shown in the gray region of each plot. During the early stages of melting, the thermal energy is transferred by conduction through the shell wall to the PCM due to the difference between the wall and the system initial temperature. Accordingly the temperature distribution is close to the solution of the Laplace equation, i.e. the isotherms have a concentric ring shape, independent of the polar angle (see left hand side of Figure 4a). It is well known that, during the early periods of the process, the dominant transport phenomenon is heat conduction, and natural convection plays a small role. For dimensionless times higher than$8.42x10^{-4}$, the isotherms begin to deviate from the concentric ring patterns indicating that natural convection starts to influence the melting process. As the melting process proceeds, the recently formed liquid phase is heated by the inner wall of the shell, changing its density and generating a buoyancy-induced flow that drives the heated fluid upward. The ascending fluid transfer its heat to the adjacent cooler fluid located in the inward direction. It is cooled down and descends adjacent to the liquid-solid interface. Hence an unsteady, counter-clockwise circulating flow is formed in the top portion of the capsule which can be illustrated by the streamline maps shown in the right side of Figures 4b to 4d. A direct result of the circulation flow pattern is the faster melting that takes place on the top portion of the solid phase and causes a change in the original spherical shape of the solid core to an oblate spheroid. This can be observed in Figures 4e and 4f. As the melting process proceeds the circulating flow grows in physical extent and the thermal energy is now transported from the inner shell wall to the liquid-solid interface primarily by natural convection. During this period, large temperature gradients are observed in the PCM liquid phase located near the inner surface of the shell. Uniform isotherms across the liquid phase (see left hand side of Figures 4g to 4i) are also observed. A possible interpretation for these observations is that the boundary layer regime has been established in the fluid flow region adjacent to the inner shell wall. Similar findings were reported by Sparrow et al. [16].

As melting continues, the solid phase shrinks in size and the circulating flow grows in physical extent and starts to develop the crescent-shaped pattern (Figures 4j and 4k). It should be noticed that the circulation speed of the convection cell decreases as the thermal equilibrium is attained. Figure 4l shows the temperature field (left) and the flow pattern (right) after the melting process is completed. Special attention should be paid to the temperature range indicated in the color maps. A well-defined crescent shaped circulation flow pattern can be observed with the circulation center close to the capsule wall. On the temperature side, a stratified temperature field is observed with high temperature gradients near the wall, especially in the lower part of the sphere. The results were found in good

agreement with the experimental and numerical results on the natural convection inside a spherical enclosure reported by Chow and Akins [17].

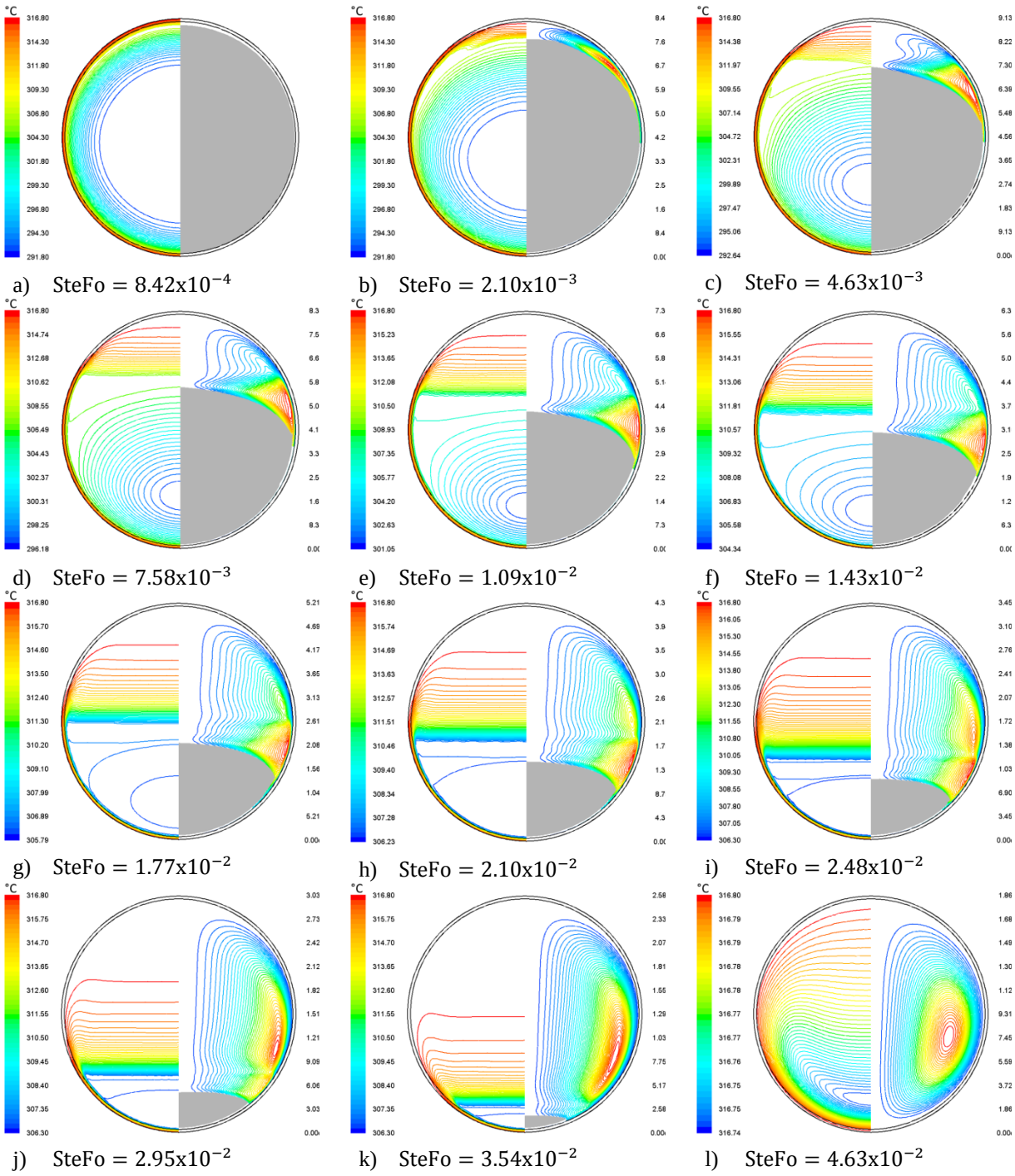

FIGURE 4. Predicted process evolution for case 13. For each subfigure, (left) isotherms, (right) PCM solid fraction in gray and stream line contours in PCM liquid phase.

The effect of the shell size on the melting rate for a constant Stefan number is presented in Figure 5(a). As expected, the larger the pellet size, the slower the pellet melts, with total melting times of 5.13, 8.10, 11.38 and 15.15 minutes

for cases 2, 6, 7 and 8 respectively. Figure 5(b) shows the predicted average heat transfer rate at the inner surface of the shell for cases 2 and 6 to 8. The heat transfer rate was found to increase with the increase of the Grashof number. Also, the heat transfer rate is proportional to the heat transfer area; therefore an increase in the available area for heat transfer causes an increase in the heat transfer rate.

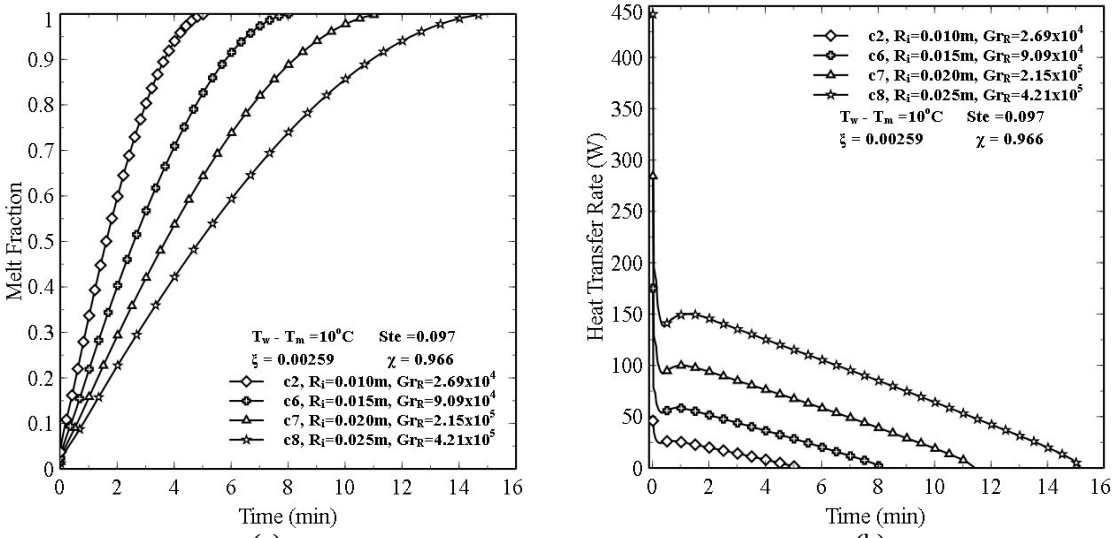

(a) (b)

FIGURE 5. Effect of the size of the shell on the melt fraction and heat transfer rate.

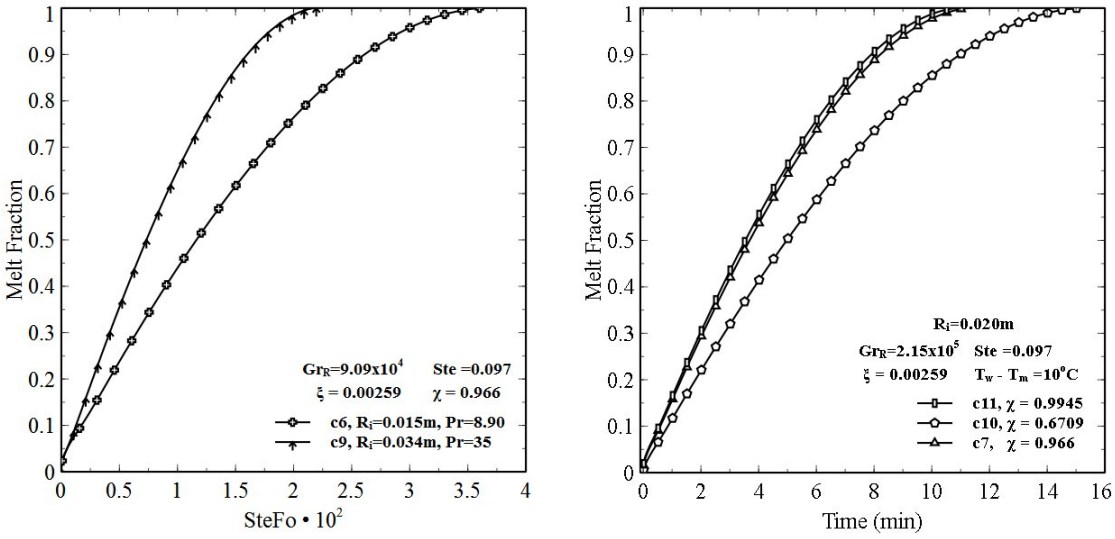

(a) (b)

FIGURE 6. Effect of the PCM and shell material properties on the melt fraction.

In order to investigate the role of Prandtl number (different phase change materials) under the same Grashof and Stefan numbers, cases 6 and 9 are compared. The material for case 9 is RT27. The Grashof and Stefan numbers were kept unchanged by manipulating the temperature difference and the pellet size. Figure 6(a) shows the predicted liquid mass fraction as a function of dimensionless time for the aforementioned cases. A significant difference in the melt fraction rate is observed. Faster rate of melting is achieved when the Prandtl number is higher. At this point, the Rayleigh number ($Ra = GrPr$), which is one of the controlling parameters in the natural convection heat transfer mode, plays a significant role. For the same Grashof number, the convective energy transport mode of a PCM with larger Prandtl number will be enhanced and consequently its melting process will be faster. The influence of the shell material thermal properties on the melt faction rate is presented in Figure 6(b). Three different shell materials have been chosen based on their thermal conductivity values in order to take into account the heat flow resistance at the

shell wall. It can be observed from Figure 6(b) that there is no significant difference in the melt fraction rate between cases 7 and 11 which correspond to metallic shells (Nickel alloy and Zinc, respectively). However a 34.1% increase in the total melting time is observed in the case 10, (Silicon Dioxide, a low thermal conductivity material) when compared to cases 7 and 11. A low thermal conductivity wall generates a high heat flow resistance and consequently a high temperature drop within the shell wall. Thermal energy requires more time to be transferred through the shell to start and continue the melting process.

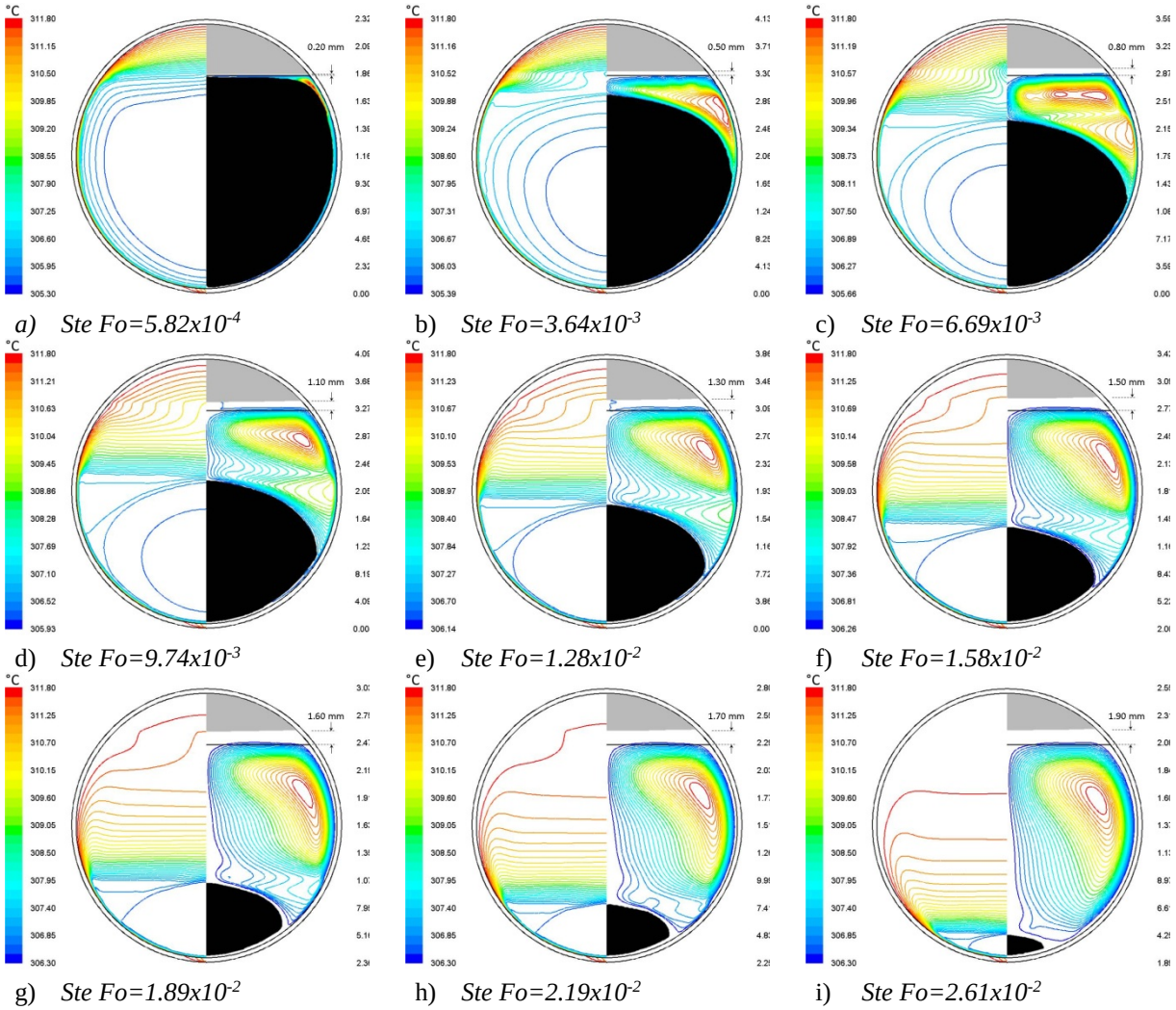

a) Ste Fo=5.82x10^{-4} b) *Ste Fo=3.64x10^{-3}* c) *Ste Fo=6.69x10^{-3}*

d) *Ste Fo=9.74x10^{-3}* e) *Ste Fo=1.28x10^{-2}* f) *Ste Fo=1.58x10^{-2}*

g) *Ste Fo=1.89x10^{-2}* h) *Ste Fo=2.19x10^{-2}* i) *Ste Fo=2.61x10^{-2}*

FIGURE 7. Predicted evolution of the melting process in partially filled capsule. For each subfigure, (left) temperature contours, (right) PCM solid fraction in black, PCM liquid streamline contours and air fraction in gray.

The evolution of the predicted isotherms, streamline contours, and PCM solid and air fraction distributions, during melting in a partially filled capsule are presented in the composite diagrams in Figure 7. The history of the process is recorded as a function of the dimensionless time defined by the product of the Stefan and Fourier numbers (SteFo). The temperature distribution of the system is presented in the left half of each circle while the right half contains the molten PCM streamline contours, and the PCM solid phase and the air fractions. At the beginning of the process, heat is transferred by conduction through the capsule wall due to the temperature difference between the wall and the initial temperature of the system. After that, thermal energy travels faster through the air due to its higher thermal diffusivity as compared to the PCM. As a result a counterclockwise buoyancy-induced recirculating flow is created in the air zone. This causes the skewed temperature contours observed in the top-left portion of Figure 7a. At the same time instant, the temperature contours of the PCM near the internal surface of the capsule, are similar to the solution of the

Laplace equation, i.e. the isotherms have a concentric ring shape, independent of the polar angle (see left side of Figure 7a). This suggests that during the early periods, the dominant transport phenomenon is heat conduction, while natural convection plays only a small role. As a result of the diffusion-controlled heat transfer process within the PCM, melting is initiated in the peripheral portion of the PCM and an axisymmetric thin layer of molten PCM is created adjacent to the inner wall of the capsule (see right side of Figure 7a). The air void is not able to provide enough heat flux to melt the top of the $NaNO_3$ at the same rate. Consequently, the upper part of the sodium nitrate remains solid. As the molten portion gets larger the density of the fluid in the vicinity of the inner surface of the shell decreases due to the temperature gradient and flows up covering the top region of the solid fraction. The combined effect of the ascending flow near the metallic shell and the descending flow in contact with the solid PCM causes an unsteady, counter-clockwise recirculating flow in the top portion of the annulus region formed between the inner shell wall and the melting interface, which is subsequently kept by natural convection due to the temperature differences between the inner wall, the air layer and the cold solid sodium nitrate. The streamline contours of the above mentioned natural convection flow can be observed at the right side of all the plots in Figure 7. This recirculating flow enhances the heating rate towards the solid, increasing the melting in this zone and the solid adopts an oblate spheroid-shape on its top (see Figures 7b and 7c). As the melting process proceeds, the solid portion shrinks in size and the recirculating flow grows in physical extent (see Figures 7d - 7f). Also, the sodium nitrate progressively fills up the pellet due to the volumetric expansion of the liquid phase, as shown in the right hand side of Figures 7g – 7i. Consequently, the air is compressed, increasing the pressure inside the pellet. In order to easily track the motion of the Air/PCM interface as a result of the thermal expansion, a horizontal line is included on the right side of all the presented plots of Figure 7, indicating the initial position of the interface and its displacement. For instance, the salt quantity inside the pellet should be carefully calculated in order to guarantee that the internal pressure does not exceed the shell mechanical strength. Even though not illustrated in these plots, after the complete melting of the solid PCM has taken place, the natural convection heat transfer continues to mix the hot fluid adjacent to the wall with the cold fluid away from the wall eventually bringing the system to an equilibrium isothermal condition.

Correlations for melt fraction and heat transfer rate were developed from numerical results for both completely and partially filled capsules. For the completely filled capsules, the melt fraction can be expressed as:

$$MF = 1 - \left[1 - \frac{FoSte^{0.33} Gr_R^{0.27} Pr^{0.37} \chi^{0.72} \xi^{-0.02}}{9.5}\right]^{1.8} \tag{7}$$

For the partially filled capsules, the following correlations were developed.

$$MF = 1 - \left[1 - \frac{FoSte^{0.37} Gr_R^{0.25}}{2.8}\right]^{2.35} \tag{8}$$

$$\frac{NuSte^{0.61}}{Gr_R^{0.27}} = \begin{cases} 0.29exp(-4.75x^{2.2}) + \sin(0.068 + 0.55x), & 0.04 \le x < 0.4 \\ 0.47exp(-0.4x^{2.0}), & 0.4 \le x \le 3.0 \end{cases} \tag{9}$$

where:

$$x = FoSte^{0.37} Gr_R^{0.25}$$

CONCLUSIONS

An axisymmetric two dimensional, transient numerical model for the coupled natural convection induced heat transfer and phase change process of sodium nitrate within a spherical enclosure has been analyzed. It was found that both the Grashof and the Stefan numbers strongly enhance the melt fraction rate of $NaNO_3$. For a fixed Grashof number ($2.6x10^4$), faster melting is achieved when the Stefan number is changed from 0.072 to 0.122. The melting time was 24.7% shorter for Case 2 (Ste=0.097), and 40.8% shorter for Case 4 (Ste=0.122) when compared to the corresponding value of case 5 (Ste=0.072). On the other hand, increasing the Grashof number from $2.69x10^4$ to $4.21x10^5$ for a fixed Stefan number also enhances the melt fraction rate. A strong influence of the Prandtl number on the melt fraction rate was found. It was found that when the shell material parameter (χ) is in the range of $0.966 - 0.994$ there is no significant difference in the total time to complete melting, under the analyzed conditions. However a 34.1% increase in the melting time is observed for $\chi = 0.67$ as compared to the previous range. Based on the fluid

flow pattern, temperature distribution and the melting interface evolution during the melting process of sodium nitrate for a fixed Stefan number (Ste=0.048), it was found that an increase in the Grashof number from $1.32x10^4$ to $2.06x10^5$ enhances the heat transfer process. As a result, the melting rate increases. Also the time averaged instantaneous heat transfer rate was found to increase with the Grashof number. A counter-clockwise recirculating cell is formed on the top portion of the region between the inner shell wall and the melting interface, which causes a more intense melting process in the upper part of the solid phase. The location of the eye of the recirculation pattern was found to be dependent on the Grashof number and moves toward the solid portion of the PCM and the inner surface of the shell as natural convection is intensified. During the early stages of the melting process, the temperature distribution is close to the solution of the Laplace equation, i.e. the isotherms have a concentric ring shape, independent of the polar angle. Later the isotherms begin to deviate from the concentric ring patterns indicating that natural convection starts to influence the melting process. Generalized correlations for liquid mass fraction and heat transfer rate during the melting process of $NaNO_3$ were developed using appropriate dimensionless parameters.

ACKNOWLEDGEMENTS

The results presented in this paper were obtained from research funded by the U.S. Department of Energy under award numbers DE-EE0003590 and DE-AR0000179 and by E.ON International Research Initiative EIRI-14-2010. The author acknowledges the technical contributions of other research team members Antonio Ramos Archibold, Jose Gonzalez-Aguilar, D. Yogi Goswami, Elias K. Stefanakos, and Manuel Romero. The research was conducted at the University of South Florida, Tampa, Florida, USA.

NOMENCLATURE

c_p	specific heat at constant pressure (J/kg K)
Fo	Fourier number $(k/\rho\, c_p)(t/R_i^2)$
Gr_R	Grashof number $(g\beta(T_w-T_m)R_i^3\rho^2/\mu^2)$
$\mathbf{g}$	gravity vector (m/s^2)
$\hbar_i$	specific enthalpy (J/kg)
κ	thermal conductivity (W/m K)
L	latent heat of fusion (J/kg)
MF	melt fraction
Nu	Nusselt number
P	pressure (Pa)
Pr	Prandtl number of the fluid $(\mu\, c_p/k)$
R_i	inner radius of the capsule (m)
Ste	Stefan number $(c_p(T_w-T_m)/L)$
t	time (s)
T	temperature (°C)
T_m	melting temperature (°C)
T_w	wall temperature (°C)
$\mathbf{u}$	velocity vector (m/s)
α	volume fraction
β	thermal expansion coefficient (1/K)
μ	dynamic viscosity (kg/m s)
ρ	density (kg/m^3)

REFERENCES

1. F.E. Moore and Y. Bayazitoglu, Journal of Heat Transfer, **104**, 19-23 (1982).
2. P.A. Bahrami and T.G. Wang, Journal of Heat Transfer, **109**(3), 806-809 (1987).
3. S.K. Roy and S. Sengupta, Journal of Heat Transfer, **109**(2), 460-462 (1987).
4. M. Bareiss and H. Beer, International Journal of Heat and Mass Transfer, **27**(5), 739-746 (1984).
5. S.K. Roy and S. Sengupta, International Journal of Heat and Mass Transfer, **33**(6), 1135-1147 (1990).

6. S.A. Fomin and T.S. Saitoh, International Journal of Heat and Mass Transfer, **42**(22), 4197-4205 (1999).
7. J.M. Khodadadi and Y. Zhang, International Journal of Heat and Mass Transfer, **44**(8), 1605-1618 (2001).
8. E. Assis, L. Katsman, G. Ziskind, and R. Letan, International Journal of Heat and Mass Transfer, **50**(9), 1790-1804 (2007).
9. F.L. Tan, International Communications in Heat and Mass Transfer, **35**, 466–475 (2008).
10. F.L. Tan, S.F. Hosseinizadeh, J.M. Khodadadi, and L. Fan, International Journal of Heat and Mass Transfer, **52**, 3464–3472 (2009).
11. S.F. Hosseinizadeh, A.A. Darzi, and F.L. Tan, International Journal of Thermal Sciences, **51**, 77-83 (2011).
12. S.F. Hosseinizadeh, A.A. Darzi, F.L. Tan, and J.M. Khodadadi, International Journal of Thermal Sciences, **63**, 55-64 (2012).
13. M.Z.M. Rizan, F.L. Tan, and C.P. Tso, International Communications in Heat and Mass Transfer, **39**, 1624-1630 (2012).
14. S.V. Patankar, *Numerical Heat Transfer and Fluid Flow* (Taylor & Francis Group, 1980).
15. V.R. Voller and C. Prakash, International Journal of Heat and Mass Transfer, **30**(8), 1709-1719 (1987).
16. E.M. Sparrow, S.V. Patankar, and S. Ramadhyani, Journal of Heat Transfer, **99**(4), 520-526 (1977).
17. M.Y. Chow and R.G. Akins, Journal of Heat Transfer, **97**, 54-59 (1975).

ICME2015

International Conference on Mechanical Engineering 2015
(ICME 2015) 18 – 20 December, 2015, Dhaka, Bangladesh

Paper ID : K-05

Engineering Education in 21st Century

Firoz Alam[1, a)], Rashid Sarkar[2, b)] and Roger La Brooy[1, c)]

[1]*School of Aerospace, Mechanical and Manufacturing Engineering, RMIT University, Melbourne, Victoria, 3083, Australia*
[2]*Department of Mechanical Engineering, Bangladesh University of Engineering and Technology, Dhaka 1000, Bangladesh*

[a)] Corresponding author: firoz.alam@rmit.edu.au
[b)] rashid@me.buet.ac.bd
[c)] roger.la-brooy@rmit.edu.au

Abstract. The internationalization of engineering curricula and engineering practices has begun in Europe, Anglosphere (English speaking) nations and Asian emerging economies through the Bologna Process and International Engineering Alliance (Washington Accord). Both the Bologna Process and the Washington Accord have introduced standardized outcome based engineering competencies and frameworks for the attainment of these competencies by restructuring existing and undertaking some new measures for an intelligent adaptation of the engineering curriculum and pedagogy. Thus graduates with such standardized outcome based curriculum can move freely as professional engineers with mutual recognition within member nations. Despite having similar or near similar curriculum, Bangladeshi engineering graduates currently cannot get mutual recognition in nations of Washington Accord and the Bologna Process due to the non-compliance of outcome based curriculum and pedagogy. This paper emphasizes the steps that are required to undertake by the engineering educational institutions and the professional body in Bangladesh to make the engineering competencies, curriculum and pedagogy compliant to the global engineering alliance. Achieving such compliance will usher in a new era for the global mobility and global engagement by Bangladesh trained engineering graduates.

BACKGROUND

Engineering graduates with global attributes are becoming increasingly important as changes in employment opportunities; demographic structure, demands for better living conditions, sustainability, and climate change are gradually becoming dominant, Alam [3], Australian Education International [2], Becker [6], ECTS [10] and ENAEE [11]. As these global challenges are directly related to engineering issues, engineering education with a global perspective has become paramount. To be effective globally, the engineering competences need to be globally relevant. An obstacle for the mobility of engineering graduates is the mutual recognition of the engineering programs (degrees), Alam et al. [4], Chowdhury et al [5 & 7]. Generally, most engineering educational institutions/universities follow the similar or near similar curricula however the recognition of engineering degrees beyond national boundary faces stiff difficulty due to the lack of mutual recognition agreement and transparency in education system, Alam et al. [4]. Graduate engineers today are increasingly needed to be international in their outlook and experience, and be prepared to operate globally. Hence, there is a growing need for the international transparency of engineering qualifications, and mechanisms to support and facilitate graduates' mobility, Alam et al. [4], Kinash et al. [17].

The rapid internationalisation of engineering curricula and engineering practices has begun in Europe, Anglosphere (English speaking) nations and Asian emerging economies through the Bologna Process and International Engineering Alliance (Washington Accord) over a decade. Both the Bologna Process and Washington Accord have introduced standardised outcome based engineering competencies and the framework for attainment of these competencies by restructuring existing and undertaking some new measures in engineering curriculum and pedagogy. Thus graduates with such standardised outcome based curriculum can move freely as professional engineers with mutual recognition within member nations, Alam et al. [4], Hanrahan [16].

The European Network for Accreditation of Engineering Education (ENAEE) was established in 2000 under the framework of Bologna Process to accredit engineering degree programs in accordance with the European Framework Standards and the Standards for Accreditation Agencies as set down by ENAEE. The ENAEE accredit Bachelor of Engineering programs as First Cycle and Master of Engineering programs as Second Cycle. In Brussels, Belgium on 19 November 2014, the thirteen professional engineering bodies signed a Mutual Recognition Agreement whereby they accept each other's accreditation decisions in respect of Bachelor and Master engineering degree programs which they accredit, EUR-ACE® Accord [21]. These 13 members are: Germany (ASIIN (Fachakkreditierungsagentur für Studiengänge der Ingenieurwissenschaften, der Informatik, der Naturwissenschaften, und der Mathematik e.V.), France (CTI - Commission des Titres d'Ingénieur), UK (Engineering Council), Ireland (Engineers Ireland), Portugal (Ordem dos Engenheiros), Russia (AEER – Association for Engineering Education in Russia), Turkey (MÜDEK – Association for Evaluation and Accreditation of Engineering Programmes), Romania (ARACIS – The Romanian Agency for Quality Assurance in Higher Education), Italy (QUACING - Agenzia per la Certificazione di Qualità e l'Accreditamento EUR-ACE dei Corsi di Studio in Ingegneria), Poland (KAUT - Accreditation Commission of Universities of Technology), Switzerland (OAQ - Organ für Akkreditierung und Qualitätssicherung der Schweizerischen Hochschulen), Spain (ANECA - National Agency for Quality Assessment and Accreditation in conjunction with IIE – Instituto de la Ingeniería de España) and Finland (FINEEC - Korkeakoulujen arviointineuvosto KKA).

Four signatories of ENAEE (Russia, UK, Turkey and Ireland) are also the full signatories of Washington Accord. Engineering graduates from these four countries have global mutual professional recognition in Europe, Anglosphere and other countries in Asia, Africa and Latin America.

Despite inheriting western nations' engineering education system, the engineering and technological qualifications obtained in Bangladesh are not readily recognized globally mainly due to the absence of National Engineering Competency Standard (NECS), its implementation processes, outcome based curriculum alignment, and the inability to become the full member of the Washington Accord. Both Washing Accord and ENAEE follow the outcome based engineering curricula where significant emphasis is put on student centred learning, work integrated learning, problem based learning, national and international experience, industry and other stakeholders' involvement. This paper discusses the importance of outcome based curricula and global mobility in order to assist countries like Bangladesh to realign their engineering curricula, develop NECS and its implementation processes and ultimately becoming a full member of the Washington Accord.

OUTCOME BASED ENGINEERING CURRICULUM/QUALIFICATION AND INTERNATIONAL RECOGNITION

Outcome Based Engineering Curriculum

The outcome based engineering education is the latest paradigm shift sweeping the education system across the world. The increasing need to produce more able, competitive and immediate work effective engineering graduates for the globalised world has led to a reform in the engineering education system whereby the learning is no longer a unilateral process and shifted its weight to be borne by the learners (students). The nucleus of outcome based learning model is a 'student centred learning' philosophy and focuses on the output (outcomes) instead of the input (taught), Rajaee et al. [19]. In contrast with traditional education, the outcome based education puts much emphasis on the learning process being actively pursued and managed by the students themselves and the lecturers are only acting as facilitators in the students' quest for knowledge. Specific and clearly defined outcomes must be described to the students so that the students will be able to set their own expectations and means to achieve the desired outcomes. As such, the role of the lecturers is to guide and provide directions for the students to navigate their own learning, Rajaee et al. [19], Engineers Australia [12].

The implementation of outcome based learning has caused a revolution in traditional academics' view and perception about the learning process and its relevant assessment. In outcome based learning, the assessment of student learning is no longer solely dependent on objective oriented exams. The assessments methods of various skills, knowledge and attitudes become diverse and various learning pedagogies are introduced to ensure the achievement of the learning outcomes. Learning tools such as problem based learning, project based learning, work integrated learning, work integrated design project, case studies, industrial placements/work experiences are some of the methods utilised to assess subjective skills acquired by the students. The defined outcomes must be specific, measureable,

achievable, realistic and time-based as it must reflect the achievement of high order learning and mastery rather than accumulation of course credits. The traditional engineering curriculum (where students are told what to do and dominated by chalk and talk) needs the restructuring of curriculum, assessment and reporting practices to be compliant with the outcome based learning curriculum. Some expected changes are:

– Curriculum Restructuring/Revision
– Innovative/Flexible Delivery Method
– Variety of Assessment and Evaluation Methods
– Collection of Evidences
– Continuous Quality Improvement (Closing the Loop)

The outcome based engineering curriculum address the following key questions to a course/subject of an engineering education program:

- What does an academic staff (lecturer) want the students to have or able to do after the completion of a course/subject successfully (Course Learning Outcomes)?
- How can an academic staff best help students to achieve these course learning objectives? (course instructional policies/course learning guides developed by the academic staff for students)
- How does the academic staff know whether students have achieved these learning outcomes/objectives (using various assessment tools)?
- If students have not achieved what are the contingency plans to do different and better for the next time? (Improvement or making the course/subject more and more effective, closing the loop)

The major advantages and benefits of the outcome based engineering curriculum are more directed and coherent curriculum where engineering graduates become more work relevant and employable to industries, organisations, agencies, higher education institutions, research organisations and other relevant stakeholders and society (more well-rounded graduates. The outcome based curriculum also allows an inevitable continuous quality improvement through the feedback provided by students, peers, industry professionals, and quality assurance authorities/ professional accreditation bodies.

Professional Recognition/Accreditation of Qualifications

In engineering education, the outcome based approach has been mandated as compulsory for accreditation of an engineering program for signatories of the Washington Accord. The Washington Accord is a mutual agreement of standards and qualifications criteria for engineering programs in the signatory countries. Bangladesh is a provisional member of Washington Accord which means that the quality of the engineering graduates in Bangladesh has to meet the internationally recognised benchmark for engineering education at par with the other signatory nations. In Bangladesh, the accreditation process is governed by the Board of Accreditation for Engineering and Technology Education (BAETE) which must oversee the accreditation of engineering programs offered by both public and private institutions across the country. According to the mutually agreed standards and qualifications, the graduates from engineering programs are expected to acquire a set of skills, knowledge and behaviours which is defined by the Washington Accord. Each signatory nation has developed a set of national standard competencies which need to be addressed by each engineering program to be professionally recognised and accredited.

In Australia, the Stage 1: Competencies was developed by the Engineers Australia (Institution of Engineers Australia) and are used by all Australian higher education institutions that offer the Bachelor of Engineering (B.Eng) degree programs (e.g., 28 Australian universities out of 39). The curriculum of bachelor of engineering programs has been realigned to address the Stage 1 Competencies in order to be professionally accredited by the Engineers Australia. The Engineers Australia developed 16 competencies are fully compatible with the International Engineering Alliance (i.e., Washington Accord signatory nations). The stage 1 competencies adopted by the Institution of Australia are the benchmark for B. Eng programs in Australia. Engineering programs must develop these competencies in an engineering program to be accredited by the Engineers Australia. Each individual subject/course within a program must address one or more competencies to address all 16 competencies of the program. These competencies are sub-grouped into 3 main categories:

a) Knowledge and Skill Base (subject specific theoretical knowledge),
b) Engineering Application Ability (capability to apply theoretical knowledge into practice to solve real world engineering problems), and

c) Professional and Personal Attributes (soft skills such as written and oral communication skills, team work and under pressure working skills, engineering ethics, sustainability, etc.). These competency sub groups are shown in Table 1.

The EA developed Stage 1 Competencies are consisted of 16 mandatory elements as shown in Table 1. The competencies and elements of competency represent the profession's expression of the knowledge and skill base, engineering application abilities, and professional skills, values and attitudes that must be demonstrated at the point of entry to practice [7]. Indicators of attainment provide insight to the breadth and depth of ability expected for each element of competency. Therefore, the indicators guide the competency demonstration and assessment processes as well as curriculum design.

An example of compulsory subjects/courses that constitute the B.Eng (Mechanical) program at RMIT University is shown in Table 2. Additionally, how these courses address the 16 EA Stage 1 Competencies from Year 1 to Year 2 (full time) is also shown.

TABLE 1. National Engineering Competencies developed by Engineers Australia, adapted from Engineers Australia [12].

Knowledge and Skill base	1.1. Comprehensive, theory based understanding of the underpinning natural and physical sciences and the engineering fundamentals applicable to the engineering discipline. 1.2. Conceptual understanding of the, mathematics, numerical analysis, statistics, and computer and information sciences which underpin the engineering discipline. 1.3. In-depth understanding of specialist bodies of knowledge within the engineering discipline. 1.4. Discernment of knowledge development and research directions within the engineering discipline. 1.5. Knowledge of contextual factors impacting the engineering discipline. 1.6. Understanding of the scope, principles, norms, accountabilities and bounds of contemporary engineering practice in the specific discipline.
Engineering Application Ability	2.1. Application of established engineering methods to complex engineering problem solving. 2.2. Fluent application of engineering techniques, tools and resources. 2.3. Application of systematic engineering synthesis and design processes. 2.4. Application of systematic approaches to the conduct and management of engineering projects.
Professional and Personal Attributes	3.1. Ethical conduct and professional accountability 3.2. Effective oral and written communication in professional and lay domains. 3.3. Creative, innovative and pro-active demeanour. 3.4. Professional use and management of information. 3.5. Orderly management of self, and professional conduct. 3.6. Effective team membership and team leadership.

TABLE 2. Program mapping against the EA Stage 1 Competency (Bachelor of Engineering- Mechanical Program at RMIT University).

Subject Titles & Credit Points		Program Learning Outcomes (PLO) as per EA Stage 1 Competencies															
		1.1	1.2	1.3	1.4	1.5	1.6	2.1	2.2	2.3	2.4	3.1	3.2	3.3	3.4	3.5	3.6
YEAR 1																	
AERO2248: Engineering, Society and Sustainability	12						TPM				TPM	TP	TP	TP			TPM
MATH2117: Engineering Mathematics C	12	TPM	TPM														
MIET2093: Computer Aided Design	12	TPM	TP	TPM					TP								
MIET2419: Mechanics and Materials 1	12	TPM	TP	TPM				TP									
MIET2421: Applied Thermodynamics	12	TPM	TP	TPM				TP									
MATH2118: Further Engineering Mathematics C	12	TPM	TPM														
MANU2095: Manufacturing Systems	12	TPM	TP	TPM				TP									
MIET2422: Fluid Mechanics of Mechanical Systems	12	TPM	TP	TPM				TP									
YEAR 2																	
MATH2124: Math & Stats for Aero, Mech & Auto	12	TPM	TPM						TPM								
MIET2370: Mechatronics Principles	12	TPM		TPM				TP	TP								
MIET2115: Mechanics and Materials 2	12	TPM	TP	TPM				TP									
MIET2134: Engineering Dynamics	12	TPM	TPM	T		TPM											
MIET2420: Mechanical Design 1	24	TP	TP	TPM		TP		TP	TPM								
Student Elective	12																
Student Elective	12																
YEAR 3																	
MIET1199: Management of Mechanical Design and Research	12	T	T	TPM	TP	TPM	TP	TP	TP	TPM	TPM	TPM	TP	TP	TP	TP	TP
MIET1071: Solid Mechanics 3	12	TP	TPM	TPM	T	T		TP	TP	TP							
MIET1076: Mechanical Vibrations	12	TP	TPM	TPM	T	T		TP	TP	TP		T	TPM				
MIET1081: Advanced Thermo-Fluid Mechanics	12	TP	TPM	TPM	T	T		TP	TP	TP			TPM				
MIET1068: Mechanical Design 2	12	TP	T	TP		TPM	TP	TP	TPM	TP	TP	T	TP		TP		
MIET1077: Mechanics of Machines	12	TPM	TPM	T	T	TP	T	TPM	T	T							
MIET1084: Finite Element Analysis	12	TP	TPM	TPM	TP	T	T	TP	TPM	TP		T	TP				
MIET2116: Engineering and Enterprise	12		T		TP	TP	TPM	T	TP	T	TPM	TP	TP	TP	TP	TP	TPM
YEAR 4																	
OENG1074: Professional Research Project 1	24	TP	TP	TP	TPM	TPM	TP	TPM	TPM	TPM	TPM	TP	TPM	TPM	TPM	TPM	TPM
OENG1075: Professional Research Project 2	24	TP	TP	TP	TPM	TPM	TP	TPM	TPM	TPM	TPM	TP	TPM	TPM	TPM	TPM	TPM
MIET2032: Renewable Energy Systems	12	TP	TPM	TP	TP	TPM		TP	TPM	TP			TP		TP		TP
MIET2006: Automatic Control (Mechanical Elective)	12	TPM	TPM	TP		TP			TP	T		T					
MIET2039: Applied Heat and Mass Transfer (Mechanical Elective)	12	TPM	TPM	TP		TP			TP	T		T					

T- Teach; P- Practice; M- Measured (the learning outcomes through assessments)

Professional Recognition/Accreditation of Qualifications

Work Integrated Learning (WIL) is an activity that integrates academic learning with its application in the workplace by combining theory with practice as part of a program. The WIL practice may be real or simulated and can occur in the workplace, at the university, online or face-to-face. Other WIL opportunities include industry placements, industry based projects and simulated work experiences. It makes a significant contribution to graduates' work and industry-readiness. WIL is a cornerstone to partnership building with the industry, community, government and other stakeholders. For all undergraduate engineering programs (B.Eng) at RMIT University, the WIL activities are compulsory and include:

Placement in Industry: A minimum of 12 weeks Industry Placements (paid or unpaid) and Cooperative Education (employment with an organisation over one or two semesters) under the supervision of a professional/practicing engineer.

Final Year Industry Sponsored Research Projects: Industrial problem solving projects or any other form of substantial projects on which students work in conjunction with industry. Usually such research projects are supervised jointly by an academic from the university and an industry profession.

Final Year non-Industry Sponsored Research Projects: A real world engineering situation is replicated/simulated in the teaching environment at RMIT University. These may take various forms depending on the specialisation engineering disciplines.

Problem Based Learning (PBL) for Work Ready Graduates

The Problem-Based Learning (PBL) is an instructional method that uses real world cases or problems as vehicles for students to acquire critical thinking and problem-solving skills. In PBL, new knowledge is acquired through solving problems. Students actively engage with the problems and develop their own understanding under the guidance of a lecturer but the lecturer does not solve the problems for students. The main philosophy of PBL is the exploratory and constructivist approach to teaching and learning. The lecturer using this approach should hold a student-centred learning concept where teaching is viewed as a means to facilitate understanding and conceptual change and or intellectual development.

The PBL is a key feature of engineering programs at RMIT University as it encourages students to draw on their creativity when solving problems and teaches students to bridge the gap between theory and practice. Students of all engineering programs including Mechanical Engineering at RMIT undertake project-based learning right from first year. As most engineers work in teams, students at RMIT undertake PBL in a team. For example, mechanical engineering students in teams undertake PBL projects such as Engineers Without Borders, Warman Design and Build, FSAE, etc. RMIT University's Advanced Manufacturing Precinct (AMP) is students' engineering design learning factory which is a unique initiative bringing together industry, RMIT expertise and students, in a collaborative environment. At AMP, industry practitioners/professional engineers work with RMIT academic staff to set projects for students, based on a real-world problem. Students work as part of a single or cross-disciplinary team to design, prototype and manufacture a solution.

OUTCOME BASED ENGINEERING CURRICULUM/QUALIFICATION AND INTERNATIONAL RECOGNITION

Now a day graduate engineers need to be international in their outlook and experience, and prepared for employable anywhere in any country. Industries, corporations, trades and businesses need to compete and collaborate on a global scale, and work across national and international borders with organisational environments being increasingly complex, dynamic and with more interdependencies. The challenges for educational institutions are to equip engineering students with the right set of skills and tools to prepare to be effective for this global environment, Greenwood [15]. The international transparency in engineering qualifications, mutual recognition of engineering qualifications, international dual awards, cross country credit transfers, short term study abroad, work integrated learning, problem based learning and industrial placement will pave the ways for the graduate engineers to be globally effective. In this regard, a number of global initiatives have been taken by many educational institutions and concerned authorities in European Union (EU), North America (USA, Canada, Mexico), Australasia (Australia, New Zealand, Fiji), South East Asia (Singapore, Malaysia, Thailand) and North Asia (Japan, Hong Kong, China, Taiwan, South Korea). A study undertaken by Buisson and Jensen [20] found that worldwide, there is a requirement to increase the internationalisation of engineering programs, curricula, content and context, as well as support for the mobility of engineering students and scholars. Several studies reported that employers emphasised the need for undergraduates to have global competence to enable them to function in the corporate environment, Dolby [9], Grandin and Hirleman 14].

Presently engineers need not only technical competencies but also an understanding of global conditions, and awareness of and sensitivity to differences in cultural environment and work ethics, Abanteriba [1]. Mobility and international experience give engineering students the opportunity to be immersed in other cultures, with exposure to different and unfamiliar situations and different approaches to problem solving, Department of Education, Employment and Workplace Relations [8]. Other benefits include "the promise of returning with an enhanced understanding of the world and its intricate web of political, economic, social and cultural relationships" (Dolby, 2008). A study by the Queensland Education and Training International (QETI) & International Education Association of Australia (IEAA) [18] reported that over 60% Australian employers consider students' international study experiences as unique and a competitive addition to a resume, while over 80% of Australian employers believe that graduates who undertake an overseas experience return to Australia with enhanced skills applicable to the workplace.

CONCLUDING REMARKS

The implementation of outcome based engineering curriculum and professional accreditation is a cyclic and continuously improvement process where the assessment of the outcomes is not the end but just the means to achieve the desired outcomes.

Effective implementation of outcome based engineering curricula and periodic professional accreditation gives opportunity for new ideas and challenges in developing an education model with improved learning outcomes and work ready graduates.

The realignment (major/minor) of existing engineering curriculum, and pedagogy will certainly make graduates work ready and programs to be accredited by the national accreditation body.

To strengthen outcome focused engineering learning, course and curriculum of engineering programs, and pedagogy should include work integrated learning (WIL), problem based learning (PBL), industry placement and stakeholders' input in program revision.

The development of robust accreditation framework comparable to the Stage 1 Competencies of a full signatory of Washington Accord will help the Board of Accreditation for Engineering and Technology Education (BAETE) to become a full signatory and graduates from BAETE accredited programs will have opportunity to work as professional engineers globally.

REFERENCES

1. Abanteriba, S., Development of strategic international industry links to promote undergraduate vocational training and postgraduate research programmes. European Journal of Engineering Education **31(3),** 283-301(2005).
2. AEI – Australian Education International, July 2009, Research Snapshot, accessed on 15 November 2015 at https://internationaleducation.gov.au
3. Alam, F. (editor) (2014), Using Technology Tools to Innovate Assessment, Reporting, and Teaching Practices in Engineering Education, IGI Global, New York, p.409, ISBN13: 9781466650114.
4. Alam, F., Alam, Q., Chowdhury, H. and Steiner, T., Transnational Education: Benefits, Threats and Challenges, Procedia Engineering **56,** 870-874 (2013)
5. Chowdhury, H., Alam, F., Biswas, S.K., Islam, M.T. and Islam A.K.M. S., Quality Assurance and Accreditation of Engineering Education in Bangladesh, Procedia Engineering **56**, 864-869 (2013)
6. Becker, F.S. (2006), Globalization, curricula reform and the consequences for engineers working in an international company, European Journal of Engineering Education **31(3),** 261(2006).
7. Chowdhury, H., Alam, F., Engineering Education in Bangladesh- An Indicator of Economic Development, European Journal of Engineering Education **37(2),** 217-228 (2012).
8. Department of Education, Employment and Workplace Relations, Australian outbound mobility: Current trends, accessed on 20 August, 2015 from www98.griffith.edu.au/dspace/bitstream/handle.
9. Dolby, N. (2008), Global Citizenship and Study Abroad: A comparative Study of American and Australian Undergraduates, Journal of Study Abroad. V. XVII, Fall 2008: 51-67.
10. ECTS - European Credit Transfer and Accumulation System, European Commission, accessed on 20 April, 2015 from ec.europa.eu/education/ects/ects_en.htm.
11. ENAEE - European Network for Accreditation of Engineering Education (2009), accessed on 24 June, 2015 from http://www.enaee.eu/enaee/presentation.htm.
12. Engineers Australia - Stage 1 Competencies for Professional Engineers (2009), accessed on 25 May 2013 from http://www.ieaust.org.au
13. European Qualifications Framework (2009), accessed on 12 April, 2015 from http://www.qca.org.uk/qca_19302.aspx.
14. Grandin, J.M. and Hirleman, E.D., Educating Engineers as Global Citizens: A Call for Action/ Report of the National Summit Meeting on the Globalization of Engineering Education, Online Journal for Global Engineering Education, 4 (1), 1-29 (2009).
15. Greenwood, P. (2008), Mobility of Engineering Professionals. Standing Committee on Education and Training Report (CET), accessed on 25 August, 2015 from http://www.wfeo.org.

16. Hanrahan, H. (2011), The Washington Accord Past, Present, Future. IEET Accreditation Training Taipei, Taiwan, September, 1-17.
17. Kinash, S., Crane, L., Knight, C., Dowling, D., Mitchell, K., McLean, M., & Schulz, M. (2014), Global graduate employability research: A report by Bond University, Gold Coast, Australia.
18. QETI & IEAA study (2006), The Attitudes and Perceptions of Australian Employers towards an Overseas Study Experience, Queensland Education and Training International, Brisbane, Australia.
19. Rajaee, N., Junaidi, E., Taib, S.N.L., Salleh, S.F. and Munot, M.A., Issues and Challenges in Implementing Outcome Based Education in Engineering Education, International Journal for Innovation Education and Research **1 (4),** 1-9 (2013).
20. Buisson, D. and Jensen, R. (2009), Stratégé - study of transparent recognition, accreditation tools and experience in a global environment, Final Project Report: January 2009, PP.1-130, Queensland University of Technology, Brisbane, Australia, 9781741072747.
21. EUR-ACE® Accord (2015), accessed on 20 October 2015 from http://www.enaee.eu/publications/eur-ace-accord/